Atmos. Chem. Phys. Discuss., doi:10.5194/acp-2016-654, 2016
Manuscript under review for journal Atmos. Chem. Phys.
Published: 12 September 2016

Atmospheric Chemistry and Physics Discussions

Impact of emissions of VOCs and NO_x on trends of ground-level O_3 in Mexico during 1993-2014: Comparison of Monterrey with Mexico City and Guadalajara

Iván Y. Hernández Paniagua[1], Kevin C. Clemitshaw[2], and Alberto Mendoza[1,*]

[1]Escuela de Ingeniería y Ciencias, Tecnologico de Monterrey, Campus Monterrey, Av. Eugenio Garza Sada 2501, Monterrey, N.L., México, 64849.
[2]Department of Earth Sciences, Royal Holloway University of London, Egham, Surrey TW20 0EX, UK.
*Corresponding author: mendoza.alberto@itesm.mx

Keywords
Air quality, emissions inventory, time series, wind-sector analysis

Abstract

In developed countries, long-term trends in O_3 have been studied extensively. However, there has been relatively little focus on economically developing countries with significant emissions of pollutant precursors. Here, the dominant role of primary emissions on regional/urban O_3 mixing ratios in Mexico is addressed. High-precision and high-frequency UV-photometic measurements of ambient O_3 have been made since 1993 at 5 sites within the Monterrey metropolitan area (MMA), in Northeast Mexico. The data sets exhibit variations on time-scales of hours, days, months and years. The O_3 diurnal cycles vary with the length of daylight, which influences photochemistry. No differences are observed in the amplitudes of the diurnal cycle (AV_d) during weekdays when fossil fuel use and combustion process are higher than during weekends, although larger AV_d are observed at polluted sites close to industrial areas. During weekdays, cycle troughs and peaks are typically recorded at 07:00 and 14:00 CDT, respectively, and during weekends, at 06:00 and 13:00 CDT, respectively.

The O_3 seasonal cycles are driven by the temporal variation of solar radiation, meteorological conditions and changes in emissions of precursors. Maximum O_3 mixing ratios are recorded in spring with minimum values in winter. The largest amplitudes of the seasonal cycles (AV_s) are typically recorded downwind of an industrial area, whereas the lowest values are recorded in a highly populated area. At all sites, AV_s declined during 1993-1998, followed by persistent increases from 1998 to 2014. Wind sector analysis show that, at all sites, the highest mixing ratios are recorded from the E and SE sectors, whilst the lowest ones are recorded in air masses from the W and NW. Wind sector analysis of mixing ratios of O_3 precursors revealed that the dominant sources of emissions are located in the industrial regions within the MMA and the surrounding area. At all sites, the largest annual increases in O_3 are for the E and SE sectors, 0.50 and 0.66 ppb yr^{-1}, respectively. Overall, during 1993 to 2014, within the MMA, O_3 has increased at an average rate of 0.22 ppb yr^{-1} (p<0.001), which is in marked contrast with a gradual decline of 0.76 ppb yr^{-1} (p<0.001) observed in the Mexico City metropolitan

Atmos. Chem. Phys. Discuss., doi:10.5194/acp-2016-654, 2016
Manuscript under review for journal Atmos. Chem. Phys.
Published: 12 September 2016

Atmospheric Chemistry and Physics Discussions

area (MCMA) for the same period. No clear trend is observed during 1996 to 2014 within the Guadalajara metropolitan area (GMA).

1. Introduction

O_3 is a secondary air pollutant formed in the troposphere via the photo-oxidation of CO and volatile organic compounds (VOCs) in the presence of NO and NO_2 ($NO + NO_2 = NO_x$) (Jenkin and Clemitshaw, 2000). Tropospheric O_3 is of concern to policy makers due to its adverse impacts on human health, agricultural crops and vegetation, and its role as a greenhouse gas despite its relatively short lifetime of around 22.3 ± 3.0 days (Stevenson et al., 2006; IPCC, 2013; WHO, 2014; Lelieveld et al., 2015). As the predominant source of OH, tropospheric O_3 controls the lifetime of CH_4, CO, VOCs, among many other air pollutants (Revell et al., 2015). In polluted regions, increased levels of O_3 are common during seasons with stable high-pressure systems and intense photochemical processing of NO_x and VOCs (Dentener et al., 2005; Xu et al., 2008; Kleanthous et al., 2014) and, to lesser extent, downward transport from the stratosphere (Wang et al., 2012). By contrast, the main removal processes for tropospheric O_3 are photolysis and reaction with NO (Atkinson, 2000; Jenkin and Clemitshaw, 2000).

O_3 increased in the Northern Hemisphere (NH) during 1950-1980s due to a rapid increase of precursor emissions derived from the industrialisation and economic growth in Europe and North America (Staehelin and Schmid, 1991; Guicherit and Roemer, 2000). O_3 precursor emissions levelled off in the 1990s in response to the introduction of air quality policies (Schultz and Rast, 2007; Butler et al., 2012), which led to the stabilisation or decrease of O_3 in some regions over North America and Europe. For example, in the Greater Area of Toronto during 2000 to 2012, O_3 levels decreased at urban sites by approximately 0.4% yr^{-1}, and at sub-urban sites by approximately 1.1% yr^{-1} as a consequence of reduced precursor emissions (Pugliese et al., 2014). Furthermore, data from the Pico Mountain Observatory in the Azores, showed significant decreases of O_3 of 0.21 ± 0.11 ppb O_3 yr^{-1}, and of CO of 0.31 ± 0.30 ppb yr^{-1} during 2000-2011 due to decreased emissions of O_3 precursors in North America and Europe (Kumar et al., 2013). From an analysis of O_3 data from 332 background stations over France during 1999-2012, Sicard et al. (2016) reported a decreasing trend of 0.12 ppb yr^{-1} caused by reduced NO_X and VOCs emissions since the 1990s.

By contrast, some regions within Europe have exhibited increasing trends in O_3 since the 1990s (Staehelin and Schmid, 1991; Oltsman et al., 2006; West et al., 2009; Logan et al., 2012; Wilson et al., 2012; Sicard et al., 2016). For instance, measurements from the Mace Head background station on the Atlantic coast of Ireland during 1987-2012 (Derwent et al., 2013), and three mountain sites in the Alps during 1991-2002 (Ordóñez et al., 2005) revealed annual increases in O_3 from 0.2 and 0.5 ppb yr^{-1} caused by increments in O_3 hemispheric background levels. An increment in tropospheric O_3 of 5-25% based on O_3 vertical profiles recorded at several sonde stations in Europe from 1970 to 1996 (Logan et al., 1999), is in good agreement with the data from the Alpine sites (Ordóñez et al., 2005). This

Atmos. Chem. Phys. Discuss., doi:10.5194/acp-2016-654, 2016
Manuscript under review for journal Atmos. Chem. Phys.
Published: 12 September 2016

Atmospheric Chemistry and Physics Discussions

78 background increase could explain the low growth rates of O_3 observed in some regions of Europe. A
79 substantial study of O_3 data recorded at 158 rural background monitoring stations in Europe carried out
80 by Wilson et al. (2012) showed significant positive annual trends in O_3 during 1996-2005 at 54% of the
81 sites, with an average overall increase of 0.16 ± 0.02 ppb yr^{-1}. Positive trends typically corresponded to
82 sites in central and north-western Europe, with negative trends observed at 11% of the sites, which
83 were located mostly in eastern and south-western Europe. It was concluded that long-term trends of
84 ambient O_3 related to reductions in NO_x and VOC were masked by factors such as changes in
85 meteorology, background O_3 and source patterns of O_3.
86
87 Tropospheric O_3 has also increased in response to reductions in precursor emissions. For example,
88 Akimoto et al. (2015) reported an increase in O_3 of 0.82-1.42% yr^{-1} for 1990-2010 at four large
89 metropolitan areas of Japan: Tokyo, Nagoya, Osaka/Kyoto and Fukoka, as a consequence of the
90 decrease of atmospheric mixing ratios of NO_x and VOCs. Sicard et al. (2016) also reported a
91 significant average increase in O_3 of 0.14 ppb yr^{-1} at urban background sites during 1999-2012 that
92 were ascribed to reduced NO_x emissions. Moreover, persistent significant increases in O_3 have been
93 observed in economically developing regions where primary emissions have increased since 1990s
94 (van der A et al., 2008; Wang et al., 2009; Chen et al., 2016), in combination with trans-boundary
95 transport of high mixing ratios of VOCs (Zhang et al., 2007; Tang et al., 2009; Akimoto et al., 2015;
96 Monks et al., 2015). This is evident, for example, in the metropolitan area of Beijing where a significant
97 increase of ca. 3.1% yr^{-1} in the tropospheric column of O_3 was observed from 2002 to 2010 (Tang et
98 al., 2009; Wang et al., 2012). Similarly, the variability of O_3 and frequency of pollution events increased
99 during 1991-2006 at the regional background station of Linan in eastern China (Xu et al., 2008). In
100 Saudi Arabia, Munir et al. (2013) reported an increasing trend in ground-level O_3 of 4.7% yr^{-1} during
101 1997-2012 in the metropolitan area of Makkah.
102
103 Long-term trends in tropospheric O_3 in Asia (Xu et al., 2008; Tang et al., 2009; Wang et al., 2012;
104 Akimoto et al., 2015), Europe (Monks, 2000; Ordóñez et al., 2005; Wilson et al., 2012; Derwent et al.,
105 2013; Sicard et al., 2016) and North America have been studied extensively (Vingarzan, 2004;
106 Pugliese et al., 2014; Monks et al., 2015). However, there has been relatively little focus on
107 economically developing countries with significant emissions of primary pollutant precursors, such as in
108 Latin America (Gallardo et al., 2012) where the few existing studies report increasing trends in O_3. For
109 example, Agudelo-Castaneda et al. (2014) observed a small increment of ca. 1.9 ppb O_3 in Porto
110 Alegre, Brazil, during 2006-2009. Similarly, Cooper et al. (2014) reported an increasing trend for 1997-
111 2013 of 0.10 ± 0.11 ppb yr^{-1} at Ushuaia in Argentina. The different rates of change in O_3 observed
112 around the globe, highlight the importance of understanding the processes that influence them, and the
113 need to examine air quality policies designed and implemented to abate emissions of O_3 precursors,
114 VOCs and NO_x.
115

Atmos. Chem. Phys. Discuss., doi:10.5194/acp-2016-654, 2016
Manuscript under review for journal Atmos. Chem. Phys.
Published: 12 September 2016

Atmospheric Chemistry and Physics Discussions

In Mexico, O_3 and other air pollutants have been studied extensively within the MCMA (Molina and Molina, 2004; Molina et al., 2010 and references therein; Song et al., 2010; Jaimes et al., 2012; Rodriguez et al., 2016). However, relatively little attention has been paid to other large metropolitan areas in the country, where $PM_{2.5}$, PM_{10}, and O_3 levels frequently exceed air quality standards (Table 1; INE, 2011; ProAire-AMM, 2008; ProAire-Jalisco, 2011; ProAire-ZMVM, 2011; Benítez-García et al., 2014). Despite several initiatives to reduce primary pollutants, since 1995, annual NO_x emissions have increased by 3.86 to 23.62 Mte NO_x yr^{-1} in the 3 largest metropolitan areas in Mexico (Fig. 1). Furthermore, since 1999 annual emissions of VOCs have increased by 12.10 to 74.86 Mte VOCs yr^{-1}, although this is only statistically significant for the MCMA due to limited data for the GMA and the MMA. At a national scale, the main source categories of NO_x and VOCs emissions are mobile (46% and 16%), point (11% and 2%), area (9% and 19%), and natural (34% and 64%), which in 2008, accounted for 2.2, 0.6, 0.4 and 1.7 Mte of NO_x, and 2.6, 0.3, 3.1 and 10.5 Mte of VOCs, respectively (SEMARNAT, 2014).

Currently, O_3 is monitored in 20 cities across Mexico (INE, 2011). During the last two decades, O_3 levels within the MCMA have decreased by ca. 33% yet still remain the highest in Mexico, followed by the GMA (the second most populated city), Leon City, and the MMA (the third most populated city) (INEGI, 2010; INE, 2011; INEGI, 2015). By contrast, O_3 levels have increased since 2000 at the GMA and MMA, exceeding by up to 80% and 50%, respectively, the official Mexican air quality standards of a 1-h average of 110 ppb O_3 and a running 8-h average of 80 ppb O_3 (NOM-020-SSA1-1993). Recent studies to address the origins and causes of these O_3 increases have focused mostly on MCMA data (Molina et al., 2010; Song et al., 2010), with less consideration of the GMA and MMA. Air quality within the MMA since 2000 was evaluated by González-Santiago et al. (2011) and by Benítez-García et al. (2014), who considered PM_{10}, and CO, NO_2, SO_2, O_3 and PM_{10}, respectively. Benítez-García et al. (2014) reported at the MMA an increase of 8 ppb O_3 during 2000-2011 from a linear regression analysis using annual averages, and several breaches per year of the 1-h and 8-h Mexican NOM. However, no previous study has analysed the O_3 ground-levels and its response to increasing precursor emissions in Mexico. This highlights the need for extensive and thorough analyses of long-term O_3 data within the MMA and other metropolitan areas, in order to better understand the underlying chemical and meteorological processes.

This study analyses the impact of increasing trends in NO_x and VOCs emissions on long-term trends in O_3 within the MMA. Long-term and high-frequency measurements of O_3 were recorded at 5 air quality monitoring stations evenly distributed within the MMA from 1993 to 2014. The data sets contain features representative of industrial, urban-background and urban monitoring sites, which allow assessment of O_3 trends and dynamics, pollutant emissions and their contribution to the atmospheric composition depending on local meteorology and air mass transport. In order to better assess photo-chemical production of O_3, total oxidants defined as ($[O_x] = [O_3] + [NO_2]$) were also considered, as O_x is not affected by the titration of O_3 with NO. Additionally, diurnal, seasonal and annual cycles of O_3 and

Atmos. Chem. Phys. Discuss., doi:10.5194/acp-2016-654, 2016
Manuscript under review for journal Atmos. Chem. Phys.
Published: 12 September 2016

O_x were evaluated in order to interpret the variations observed. The influence of air mass origin on O_3 annual growth rates has also been evaluated. Finally, long-term trends in O_3 and precursor emissions are compared with those observed within the MCMA and GMA.

2. Methodology

2.1 Monitoring of O_3 in the Monterrey Metropolitan Area (MMA)

The MMA (25°40'N, 100°20'W) is located around 720 km N of Mexico City, some 230 km S of the US border in the State of Nuevo Leon (Fig. 2a). It lies at an average altitude of 500 m above sea level (m asl) and is surrounded by mountains to the S and W, with flat terrain to the NE (Fig. 2b). The MMA covers an area of around 4,030 km^2, is the largest urban area in Northern Mexico, and is the third most populous in the country with 4.16 million inhabitants, which in 2010, comprised 88% of the population of Nuevo Leon State (INEGI, 2010). The MMA is the second most important industrial area with the highest gross domestic product per capita in Mexico (Fig. 2c). Although the weather rapidly fluctuates on a daily time-scale, the climate is semi-arid with an annual average rainfall of 590 mm, and an annual average temperature of 25.0°C with hot summers and mild winters (ProAire-AMM, 2008; SMN, 2016).

Air mass back-trajectories (AMBT) were calculated using the HYSPLIT model v.4 (NOAA Air Resources Laboratory (ARL); Stein et al., 2015), with the Global NOAA-NCEP/NCAR reanalysis data files on a latitude-longitude grid of 2.5 degrees, downloaded from the NOAA ARL website (http://ready.arl.noaa.gov/HYSPLIT.php). HYSPLIT frequency plots of 96-h AMBT were constructed for every 6 h during the year 2014 with an arrival altitude of 100 m above ground level. Figure 3 shows that the MMA is highly influenced by anti-cyclonic, easterly air masses that arrive from the Gulf of Mexico, especially during summer.

Figure 4 shows the frequency count of 1-h averages of wind direction by site and season within the MMA during 1993-2014. At all sites, apart from OBI, the predominant wind direction is clearly E, which occurs between 35-58% of the time depending on season. These air masses are augmented by emissions from within the MMA that are prevented from dispersing by the surrounding mountains. On average, the highest wind speeds are observed during summer. By contrast, calm winds of ≤ 0.36 km h^{-1} (0.1 m s^{-1}) occurred less than 2% of the time at all sites, most frequently in winter, and least frequently in summer.

Tropospheric O_3, 6 additional air pollutants (CO, NO, NO_2, SO_2, PM_{10}, and $PM_{2.5}$) and 7 meteorological parameters (wind speed (WS), wind direction (WD), temperature (Temp), rainfall, solar radiation (SR), relative humidity (RH) and pressure) have been monitored continuously since November 1992 at 5 stations that form part of the Integral Environmental Monitoring System (SIMA) of the Nuevo Leon State Government (Table 2; SDS, 2016). From November 1992 to April 2003, and in accordance with EPA, EQOA-0880-047, Thermo Environmental Inc. (TEI) model 49 UV photometric analysers were

Atmos. Chem. Phys. Discuss., doi:10.5194/acp-2016-654, 2016
Manuscript under review for journal Atmos. Chem. Phys.
Published: 12 September 2016

Atmospheric Chemistry and Physics Discussions

used to measure O_3 with stated precision less than ±2 ppb O_3 and a detection limit of 2 ppb O_3. Similarly, in accordance with RFNA-1289-074, TEI model 49 NO-O_3 chemiluminescence detectors were used to measure NO-NO_2-NO_x with stated precision less than ±0.5 ppb NO, and a detection limit of 0.5 ppb NO. In May 2003, replacement TEI model 49C O_3 and model 49C NO-NO_2-NO_x analysers were operated as above, with stated precision better than ±1 ppb O_3 and ±0.4 ppb NO, respectively, and detection limits of 1 ppb O_3 and 0.4 ppb NO, respectively. Calibration, maintenance procedures and quality assurance/quality control (QA/QC) followed protocols established in the Mexican standards NOM-036-SEMARNAT-1993 and NOM-156-SEMARNAT-2012. The SIMA dataset has been validated by the Research Division of Air Quality of the Secretariat of Environment and Natural Resources.

2.2 Monitoring of O_3 in the Mexico City Metropolitan Area (MCMA)

The MCMA is located in Central Mexico (19°30'N, 99°02'W) and covers an area of around 9,500 km^2 (Fig. 2a). It lies at an average altitude of 2,500 m asl and is surrounded completely by mountains. The MCMA has a population of 20.1 million inhabitants, which makes it the most populous city in Mexico and third in the world (INEGI, 2010). The climate is mild with an annual average temperature of 12-16°C and annual average rainfall of 820 mm. For decades, air pollution emissions in the MCMA, primarily from the industrial, transport and services sectors, resulted in air quality that was and is considered to be very poor by comparison with other large cities in Mexico and with other megacities worldwide (INE, 2011).

Within the MCMA, air quality monitoring is carried out by the Atmospheric Monitoring System of Mexico City (SIMAT), which measures 7 criteria air pollutants (O_3, SO_2, NO, NO_2, CO, PM_{10} and $PM_{2.5}$), and 5 meteorological parameters (WS, WD, Temp, RH and UV-SR). SIMAT currently operates a network of 34 stations to monitor air quality, and 15 stations to record meteorological parameters (SEDEMA, 2016). Data are stored on a central server as hourly averages pending validation by SIMAT. The validated SIMAT data archive comprises hourly measurements of the above 7 criteria air pollutants and 5 meteorological parameters from January 1986 to December 2014. It is managed by the Government of Mexico City, and data were downloaded from their web site (http://www.aire.df.gob.mx/default.php).

2.3 Monitoring of O_3 in the Guadalajara Metropolitan Area (GMA)

The GMA is located NW of Mexico City (20°39'N, 103°21'W; Fig. 2a), covers an area of 3,450 km^2, and with a population of 4.5 million inhabitants, is the second most populous urban area in Mexico (INEGI, 2010). It is located at an average altitude of 1,550 m asl. The climate is mild with dry springs and wet summers. The annual average temperature is 20.9°C and annual average rainfall is 1,030 mm. The GMA experiences occasional pollution events due to local emissions from automobiles, industry, and commercial and services activities (INE, 2011; SEMADET, 2014). Air quality is monitored within the GMA by the Atmospheric Monitoring System of the Jalisco State (SIMAJ). SIMAJ currently operates 10 stations, which report hourly data for 6 criteria pollutants (CO, NO, NO_2, O_3, PM_{10}, and SO_2) and four meteorological parameters (WS, WD, Temp and RH) (SEMADET, 2016). The SIMAJ data archive

Atmos. Chem. Phys. Discuss., doi:10.5194/acp-2016-654, 2016
Manuscript under review for journal Atmos. Chem. Phys.
Published: 12 September 2016

Atmospheric Chemistry and Physics Discussions

contains hourly data recorded from January 1996 to December 2014. It is managed by the Environment and Territorial Development Secretariat of the Jalisco State government, with data downloaded from their web site (http://siga.jalisco.gob.mx/aire/Datos.html).

2.4 Analysis of data

SIMA, SIMAT and SIMAJ instrumentation recorded O_3 data every minute, which were then validated and archived as 1-h averages. Total SIMA O_3 data capture by year and site are shown in Fig. 5. Data capture averaged during 1993-2014 ranged from 82.6% at GPE to 93.3% at SNB, with data capture <50% during 1998-2000 at GPE, in 1998 at SNN, and in 1999 at OBI. A threshold of 75% data capture was defined to consider data valid and representative (ProAire-AMM, 2008; Zellweger et al., 2009; Wilson et al., 2012). All data were processed with hourly averages used to determine daily averages, which were used to calculate monthly averages, from which yearly averages were obtained.

The SIMA, SIMAT and SIMAJ O_3 data sets were analysed extensively using the *openair* package for R software (Carslaw and Ropkins, 2012; R Core Team, 2013; Carslaw, 2015). Long-term O_3 trends were calculated with the MAKESENS 1.0 macro (Salmi et al., 2002), with O_3 time-series decomposed into trend, seasonal and residual components using the Seasonal-Trend Decomposition technique (STL; Cleveland et al., 1990). Statistical analyses were carried out with SPSS 19.0 with the Kalman Smoother (KS) used to provide minimum-variance, unbiased linear estimations of observations and to impute missing O_3 data to satisfy the STL (Reinsel, 1997; Durbin et al., 2012; Carslaw, 2015). Overall, statistical seasonal auto-regressive and moving averages with annual seasonal components were employed.

In order to carry our seasonal analyses of data, seasons were defined according to temperature records in the NH, as described previously (Hernandez-Paniagua et al., 2015): winter (December-February), spring (March-May), summer (June-August) and autumn (September-November). Wind-sector analyses of data were performed by defining 8 wind sectors each of 45° starting from 0° ± 22.5°. The lower bound of each sector was established by adding 0.5° to avoid data duplicity. Data were assigned to a calm sector when wind speed was ≤ 0.36 km h^{-1}.

3. Results and Discussion

3.1 Continuous records and trend of daily maxima of O_3 and O_x

Figure 6 shows the complete data set of 1-h averages and monthly averages of O_3 recorded at the 5 monitoring stations within the MMA from January 1993 to December 2014. The highest O_3 1-h averages were observed at SNB and STA, and are likely to arise from short-range transport and large upwind emissions of O_3 precursors from vehicles and industries. The highest O_3 mixing ratios (1-h averages) are typically observed in April (spring), with lowest values usually recorded in December and January (winter). Table 3 summarises the minimum, maximum, mean (average) and median O_3 mixing ratios recorded. The highest mixing ratios recorded were 186 ppb O_3 at GPE in 1997, 146 ppb O_3 at

Atmos. Chem. Phys. Discuss., doi:10.5194/acp-2016-654, 2016
Manuscript under review for journal Atmos. Chem. Phys.
Published: 12 September 2016

Atmospheric Chemistry and Physics Discussions

SNN in 2004, and 224 ppb O_3 at SNB in 2001. At OBI and STA, the highest O_3 mixing ratios were both recorded on June 2, 1993: 182 ppb at 12:00 CDT at OBI, and 183 ppb at 13:00 CDT at STA. Annual averages varied from 14 ± 14 ppb O_3 at OBI in 2001 to 31 ± 23 ppb O_3 at SNB in 1993.

Reaction with NO rapidly converts O_3 to NO_2, and therefore mixing ratios of odd oxygen (O_x = O_3 + NO_2) were calculated for each hour during 1993-2014 at the 5 sites within the MMA (Table S1). Minimum values of O_x ranged from 0 ppb at SNB and at STA in 2002 and 2001, respectively, to 13 ppb at OBI in 2007. Maximum values of O_x ranged from 89 ppb to 330 at GPE in 2000 and at OBI in 1993, respectively. Annual averages varied from 19 ± 16 ppb at SNN in 2002 to 51 ± 27 ppb at OBI and at STA in 2001 and 2006, respectively. The highest values of O_x were observed at OBI during 1993-2002, which coincided with the largest mixing ratios of NO_2 that were likely dominated by vehicle emissions. Since 2003, the highest O_x mixing ratios recorded at STA were likely due to increasing upwind NO_x and VOCs emissions mostly from industries (INE, 1997; SEMARNAT, 2011; 2014, SDS, 2015). As for O_3, O_x exhibits a seasonal cycle with the highest values in spring and lowest values in winter.

Figure 7 shows de-seasonalised, long-term trends of maximum daily 1-h averages of O_3 and O_x. Overall, significant increasing trends of 0.34 to 0.79 ppb O_3 yr^{-1} are observed at GPE and SNN, respectively. The large annual increase observed at SNN is likely influenced by increases in localised industrial emissions of O_3 precursors and constant urban growth. The trend at STA may be masked by local import of O_3 and poor dispersion of O_3 precursors, although further studies are required (ProAire-AMM, 2008; SDS, 2015). The maximum daily mixing ratios of O_x show significant increasing trends of 0.18, 0.62 and 0.43 ppb O_x yr^{-1} at GPE, SNN and SNB, respectively. By contrast, decreasing trends of -0.49 and -0.56 ppb O_x yr^{-1} respectively, are seen at OBI and STA.

For GPE, SNN and SNB, maximum daily 1-h averages trends in O_3 and Ox are all positive, for STA both trends are negative although not significant, and at OBI, the trend for O_3 is positive whereas that for O_x is negative. The negative trends in O_x at OBI and STA are likely to be related to decreased NO_x emissions due to improved exhaust catalyst technology in an expanding fleet of new vehicles (Pugliese et al., 2014; INEGI, 2015). Indeed, in the area of OBI, NO_x emissions have decreased significantly since 2000 (ProAire-AMM, 2008; SDS, 2015).

3.2 O_3 daily cycles

Figure 8 shows daily profiles of O_3, O_x, NO, NO_2, NO_x, and SR averaged over the 5 sites within the MMA. O_3 generally dips during rush hour by reaction with NO, which occurs around 07:00 in spring and summer and 08:00 in autumn and winter. O_3 generally peaks around 13:00 in spring, 12:00 in summer (co-incident with SR), and about 14:00 in autumn and winter. Similar profiles are observed for O_3 being in an anti-phase cycles of NO_2 mixing ratios (r=0.93 (winter) to 0.97 (summer), p<0.05 in all seasons). Despite differences of 1 to 3 hours in the timing of the O_3 dips and peaks shown in Figure 8, they coincide broadly with those observed elsewhere in the NH. For example, O_3 daily maxima occur

Atmos. Chem. Phys. Discuss., doi:10.5194/acp-2016-654, 2016
Manuscript under review for journal Atmos. Chem. Phys.
Published: 12 September 2016

between 13:00 and 15:00 LST at 4 metropolitan areas of Japan (Akimoto et al., 2015), 11 stations in the Iberian Peninsula (Domínguez-López et al., 2015), the metropolitan area of Toronto, Canada (Pugliese et al., 2014), and at 3 stations in Cyprus (Kleanthous et al., 2015).

Normalised O_3 daily profiles were constructed to analyse seasonal variations at the 5 monitoring sites within the MMA (Fig. 9). Daily amplitude values (AV_d) were calculated by subtracting the lowest normalised values from the highest normalised values. The lowest AV_d values occur in winter, consistently for SNN with 33.5 ppb O_3. These are associated with the inflow of NE and E air masses laden with VOC and NO_x precursor emissions, that are transported to OBI and then on to STA, where they become stagnated by the surrounding mountains. Consequently, the largest AV_d are observed in summer at all 5 sites, particularly for STA with a value of 56.5 ppb O_3. In Toronto, for example, Pugliese et al. (2014) observed that O_3 maxima were enhanced by photochemical processing of air masses from polluted wind sectors, whereas O_3 maxima were decreased in cleaner air masses. O_3 daily profiles and AV_d similar to those for the MMA were observed at Linan in China from 1995 to 2006 (Xu et al., 2008) with variability in AV_d ascribed to increasing emissions of O_3 precursors, particularly NO_x.

3.3. O_3 seasonal cycles within the MMA from STL data

Monthly averages of O_3 and SR for the MMA during 1993-2014 were filtered with the STL technique to de-compose the data into seasonal, secular trend and residual components (Cleveland et al., 1990; Carslaw and Ropkins, 2012). Figure 10 shows the seasonality of O_3 with spring-time maxima, winter minima, and a good correlation with SR (r= 0.72, p<0.001) (Lelieveld and Dentener, 2000). This behaviour agrees well with O_3 spring maxima and winter minima characteristic of many NH mid-latitude sites (Monks, 2000; Vingarzan, 2004, Monks et al., 2015, and references therein). Within the MMA, O_3 minima occur throughout 1993-2014 in December except for 1993, 2000 and 2007, when delayed until January. By contrast, O_3 maxima were observed during 1993-2014 in April except for 2000-2004, 2007, 2010 and 2014 when in May. Bigi and Harrison (2010) reported O_3 minima in December and maxima in June for the urban location of North Kensington, London.

Figure 10 shows downward spikes in the seasonal cycles of O_3 during July-August and are due to high wind speeds that disperse O_3 precursors, increase the boundary layer height, and reduce rainfall (ProAire-AMM, 2008). Xu et al. (2008) reported similar O_3 seasonal behaviour for Linan in eastern China with maxima occurring in May, followed by a trough in July and a second peak in October. This behaviour was attributed to the Asian summer monsoon, which brings maritime clean air to the region and constant rainfall. Within the MMA, during late summer and early autumn O_3 levels are comparable with those in spring, although suppressed during frequent rain storms.

An average seasonal amplitude value (AV_s) of 15.1 ± 2.97 (1σ) ppb O_3 for the MMA data from 1993-2014 was calculated from STL filtered data. The lowest AV_s was 10.3 ppb O_3 in 1998, with the largest

Atmos. Chem. Phys. Discuss., doi:10.5194/acp-2016-654, 2016
Manuscript under review for journal Atmos. Chem. Phys.
Published: 12 September 2016

Atmospheric Chemistry and Physics Discussions

value of 19.0 ppb O_3 observed in 2014. AV_s for the MMA are slightly lower than those calculated at the North Kensington site in London, which ranged from ca. 7.0 ppb O_3 in 2000 to ~25.5 ppb O_3 in 2005 (Bigi and Harrison, 2010), presumably due to lower emissions of NO_x and VOCs within the MMA (SDS, 2015). The average AV_s for the MMA agrees well with that of 10.5 ppb O_3 recorded during 2004-2005 at the Pico Mountain Observatory in Portugal (Kumar et al., 2013). Thus despite trends of increasing O_3 precursor emissions within the MMA, AV_s lie within the range of those recorded at sites in the USA and Western Europe that are highly influenced by transport of O_3 and precursors from regions with reduced emissions.

Figure 11 shows long-term trends of O_3 AV_s for the 5 MMA sites during 1993-2014. Significant decreases in O_3 AV_s are observed during 1993-1997 for GPE and SNB and, during 1993-1998 for SNN, OBI and STA. By contrast, significant increases in O_3 AV_s are observed for all sites from 1998. The declining trends range from -0.93 ppb O_3 yr^{-1} for GPE to -2.32 ppb O_3 yr^{-1} for SNN, with increasing trends of 1.19 ppb O_3 yr^{-1} at OBI to 2.07 ppb O_3 yr^{-1} at GPE. A plausible explanation for such changes is the economic crisis experienced in Mexico during 1994-96 (Tiwari et al., 2014). Although emissions inventories provide relatively little information, it is suggested that decreased O_3 precursor emissions of VOCs and NO_x were responsible for the changes observed.

3.4. Long-term trends of O_3 within the MMA during 1993-2014

Long-term trends of O_3 during 1993-2014 were calculated using the Mann-Kendall test and Sen's estimate (Salmi et al., 2002) for the 5 sites within the MMA. Figure 12 shows calculated long-term trends of annual averages derived from de-seasonalised monthly averages. Overall, O_3 mixing ratios show significant increasing trends at all sites except for STA, where no trend was observed despite exhibiting the highest mixing ratios recorded. Significant trends ranged from 0.12 ppb O_3 yr^{-1} at SNB to 0.29 ppb O_3 yr^{-1} at OBI. Note that if trends are segmented and considered only after the decline in 1995, the only significant change is that the O_3 growth rate at SNN would increase to 0.28 ppb O_3 yr^{-1}. The increasing trend at SNN is likely caused by increasing emissions of NO_x and VOCs from the industrial area, which is in agreement with data reported in the National Emissions Inventories (INE, 1997a,b; SEDEMA, 1999; 2001; 2003; 2004; INE-SEMARNAT, 2006; SEDEMA, 2006; 2008; 2010; SEMARNAT, 2011; SEDEMA, 2012; 2013; SEMARNAT, 2014; SDS, 2015.).

At OBI, the significant increasing trend of 0.24 ppb O_3 yr^{-1} contrasted with a decreasing trend of -0.51 ppb NO_2 yr^{-1}. These opposite trends may arise from increasing emissions of VOCs but decreasing NO_x emissions because the MMA is VOC-sensitive (Sierra et al., 2013), which can be confirmed by decreasing mixing ratios of -0.57 ppb NO_x yr^{-1} and -0.43 ppb NO_2 yr^{-1}, (both at p<0.001) at OBI. The vehicular fleet within the city centre is comprised mostly of recent model automobiles fitted with improved catalyst technology that could contribute to decreased NO_x levels, which was also observed in the Greater Toronto Area (Pugliese et al., 2014). By contrast, higher NO_x emissions from older

Atmos. Chem. Phys. Discuss., doi:10.5194/acp-2016-654, 2016
Manuscript under review for journal Atmos. Chem. Phys.
Published: 12 September 2016

Atmospheric Chemistry and Physics Discussions

vehicles, including the transport fleet, diesel buses and large trucks that are usually driven on motorways located on periphery of the MMA, could explain the O_3 mixing ratios at SNN and SNB.

Significant increasing trends of 0.22 ppb O_x yr^{-1} at GPE, 0.30 ppb O_x yr^{-1} at SNN and 0.38 ppb O_x yr^{-1} at SNB are similar to those of O_3, and may be ascribed to increased emissions of NO_x and VOCs as seen in Fig. 1. Moreover, following the economic crisis in Mexico during 1994-96, annual averages of petrol sales in the Nuevo Leon state increased linearly from 1996 to 2008 at a rate of 95,820 m^3 petrol yr^{-1} (r = 0.95) (SENER, 2015). As for petrol sales, registered vehicles in Nuevo Leon show significant variations between 1993 and 1996, and a linear annual growth rate of 100,000 vehicles yr^{-1} (r=0.99) from 1997 to 2014, which is in agreement with the increasing trend for vehicular emissions reported in the Emissions Inventories (INEGI, 2015; SDS, 2015). By contrast, at STA non-significant trends were identified in O_3 and O_x, which is likely due to the accumulation of pollutants in the vicinity of STA in stagnant air masses. This might also explain the high O_3 and PM_{10} levels reported by González-Santiago et al. (2011) and Benítez-García et al. (2014), and the significant decreasing trend of NO_2. However, continued monitoring at OBI and STA is required to more accurately assess trends in O_3, O_x and NO_2, and to understand more fully the processes that influence them.

Although there are no studies to date of long-term trends in O_3 apart from those within the MCMA in Mexico, significant increasing trends of ambient O_3 such as detected within the MMA have also been observed elsewhere in the NH. For example, Bigi and Harrison (2010) reported an steady increase of around 15 μg m^{-3} O_3 in North Kensington, London during 1996-2008 (ca. 0.5 ppb O_3 yr^{-1}), which was attributed to the long-term decrease in NO emissions. By contrast, within the MMA, NO_x emissions and the VOC:NO_x ratio have increased at a constant rate during 1999-2013, which may help explain the lower growth rates of O_3. O_3 growth rates within the MMA correspond to 19 - 38 % of those at Makkah City in Saudi Arabia from 1998 to 2012 of ca. 0.79 ppb O_3 yr^{-1} (Munir et al., 2013), which are due to increasing NO:NO_2 ratios both at Makkah and at MMA. O_3 growth rates similar to those recorded within the MMA of between 0.22 - 0.37 ppb O_3 yr^{-1} (p<0.05) were recorded at four urban areas in Japan during 1990-2010 (Akimoto et al., 2015), and are ascribed to trans-boundary transport of O_3 and a decrease of the NO tritation effect. Finally, the non-significant increasing trend of 0.11 ppb O_3 yr^{-1} at Agia Marina in Cyprus is influenced by regional transport rather than local emissions of VOCs and NO_x (Kleanthous et al., 2015), unlike within the MMA where both processes have a role.

3.5 O_3 growth rates by wind sector within the MMA

Long-term trends in O_3, O_x and NO_x recorded within the MMA were determined by wind sector. Data were split into 8 wind sectors with the Mann-Kendall test and Sen's estimate used to calculate annual growth rates. Table 4 shows that annual O_3 growth ranged from -0.06 ppb O_3 yr^{-1} for SNN and SW, to 0.66 ppb O_3 yr^{-1} for OBI and SE. The largest and most significant O_3 growth rates are seen for the E and SE sectors, whereas the lowest growth rates correspond to the W sector. Similarly, the largest O_x growth rates of 0.78 ppb O_x yr^{-1} at GPE, SNN, and 0.55 ppb O_x yr^{-1} at SNB are observed for the E and

Atmos. Chem. Phys. Discuss., doi:10.5194/acp-2016-654, 2016
Manuscript under review for journal Atmos. Chem. Phys.
Published: 12 September 2016

Atmospheric Chemistry and Physics Discussions

427 SE sectors. By contrast, significant decreasing trends of 0.48 ppb O_x yr^{-1} and 1.52 ppb NO_x yr^{-1} were
428 calculated for the SW sector at OBI, whereas non-significant trends were apparent at STA. The
429 observed growth rates highlight the dominant contribution of local industrial emissions of O_3 precursors
430 and the role of regional-scale transport of O_3: largest growth rates are observed at SNN and OBI that
431 are downwind of significant industrial emissions.
432
433 **3.6. Comparison of MMA O_3 weekly profiles with those at MCMA and GMA**
434 Hourly O_3 data were used to construct weekly averaged profiles for the MCMA from 1993 to 2014, and
435 for the GMA from 1996 to 2014. Figure 13 compares weekly O_3 cycles within the MMA with those for
436 the MCMA and GMA. In each case, and consistent with observations in other major NH urban areas
437 (Qin et al., 2004; Song et al., 2008; Akimoto et al., 2015), the lowest O_3 mixing ratios occur before
438 sunrise with peak values apparent after mid-day. It should be noted that the peak value for the MCMA
439 occurs an hour or so earlier than for the MMA and GMA and is attributed to accelerated photo-
440 chemical production of O_3 during late morning (Volkamer et al., 2010). As might be anticipated, larger
441 AV_d of 76.9 ± 1.6 ppb O_3 were observed for the MCMA than for the GMA (46.1 ± 1.0 ppb O_3) and MMA
442 (37.6 ± 0.4 ppb O_3), and as seen in Fig. 1, appear to be related to the relative emissions of the O_3
443 precursors, VOCs and NO_x. However, as shown in Fig. 13, there appear to be no significant
444 differences (p>0.05) at any of the metropolitan areas between O_3 AV_d during weekends and weekdays
445 as was reported for the MCMA by Stephens et al. (2008). This lack of a weekend effect is understood
446 to be likely due to weekday O_3 production being limited by VOCs and inhibited by NO_x (Song et al.,
447 2008; Monks et al., 2015); reductions in VOCs emissions alone could reduce O_3 mixing ratios, whereas
448 reductions in NO_x may lead to increased O_3 mixing ratios (Song et al., 2008; Wolff et al., 2013).
449
450 **3.7. Long-term trends at MCMA, GMA and MMA from 1993 to 2014**
451 Annual averages of O_3 for sites within the MCMA and GMA were calculated as for the MMA sites, and
452 are plotted in Fig. 14. The data suggest that within the MCMA, O_3 decreased by 18.7 ppb during 1993-
453 2014 and within the GMA O_3 decreased by 14.4 ppb O_3 during 1996-2014. By contrast, an apparent
454 increase in O_3 within the MMA of 0.4 ppb O_3 is seen during 1993-2014. The observed decline in O_3 at
455 MCMA in the present study agrees well with the reported reductions of 20 ppb O_3 during 1991-2011
456 (Jaimes et al., 2012), and 6 ppb O_3 during 2000-2011 (Benítez-García et al., 2014).
457
458 However, by contrast with our findings, Benítez-García et al. (2014) report an increase of 12 ppb O_3
459 within the GMA during 2000-2011 and an increase of 8 ppb O_3 within the MMA from 2000 to 2011.
460 Such differences in both the sense and magnitude of O_3 trends are likely due to the different periods
461 evaluated; the large annual variability observed within the GMA and MMA could certainly affect the
462 overall change estimated. This is evident when analysing the variation in annual averages of O_3 (ΔO_3),
463 within a particular period: from 10.2 ppb O_3 for 2012-2013 to -2.2 ppb O_3 for 2004-2005 within the
464 GMA, and from 3.5 ppb O_3 for 2000-2001 to -4.1 ppb O_3 for 2002-2003 within the MMA, respectively.
465

Atmos. Chem. Phys. Discuss., doi:10.5194/acp-2016-654, 2016
Manuscript under review for journal Atmos. Chem. Phys.
Published: 12 September 2016

Atmospheric Chemistry and Physics Discussions

Long-term trends of O_3 within the MMA, MCMA and GMA are shown in Fig. 14. Within the MMA, a significant increasing trend of 0.20 ppb O_3 yr^{-1} is observed during 1993-2014, within the MCMA a significant decreasing trend of -0.71 ppb O_3 yr^{-1} may be seen during the same period, while within the GMA, a non-significant trend of -0.09 ppb O_3 yr^{-1} is evident during 1996-2014. Such trends in O_3 reflect the long-term trends in VOC and NO_x emissions (Fig. 1). Thus, whereas O_3 precursor emissions have reduced from early 2000s within the MCMA, emissions within the GMA and MMA have continued to increase despite the introduction of new abatement policies. Finally, the results obtained here demonstrate the merits of the assessment and analysis of long-term continuous data for air quality and air pollutant emissions, with continued monitoring required to confirm the observed positive trend and growth rate of O_3 within the MMA and, to better understand the changes in regional and urban O_3.

3.8 Compliance with the 1-h and 8-h O_3 Mexican Standards

In an effort to improve air quality within the MMA, several evaluations of compliance against air quality standards have been conducted by the local government, together with compilations of emissions inventories (ProAire-AMM, 2008). In Mexico, the running 8-h average standard of 80 ppb O_3 is considered to be breached if more than 4 exceedances occur in a calendar year (NOM-020-SSA1-1993). Since 19 Oct 2014, there have been new maximum permitted levels of a 1-h average of 95 ppb O_3 and a running 8-h average of 70 ppb O_3, respectively (NOM-020-SSA1-2014). Table 5 shows that both standards are exceeded within the MMA, most frequently at STA, with the fewest breaches at SNN, which has the largest growth rate of O_3, and at GPE.

The number of exceedances has increased in recent years, except at STA where no pattern is observed, which is in good agreement the observed trends of increasing O_3 mixing ratios. When exceedances were tested for linear trends, SNN and SNB showed significant growing trends at $p<0.05$ both in the 1-h average and 8-h running average standards. This would suggest that according to the long-term trends in O_3 calculated at the MMA, the number of exceedances of the standards will increase as result of increasing precursor emissions from the industrial and transport sectors. Therefore, it is recommended that more stringent emission controls are introduced in order to improve air quality within the MMA.

4. Conclusions

The impact of increasing NO_x and VOCs emissions over O_3 long-term trends in the MMA, MCMA and GMA has been addressed by the first time in this study. Continuous high-frequency and high-precision O_3 data recorded during 1993-2014 at 5 sites within the MMA and 29 sites within the MCMA, and during 1996-2014 at 10 sites within the GMA, were used to calculate long-term trends. Within the MMA, the greatest mixing ratios of O_3 were recorded at OBI in E and SE air masses, representing transport of precursors from industrial sources, dominant in the periphery of the MMA. The lowest O_3 mixing ratios were recorded at SNN, and for all sites were observed for the W and SW sectors, where air masses travel from central Mexico over 100-300 km of semi-arid region sparsely populated.

505 Maximum daily 1-h values of O_3 and O_x increased significantly at GPE, SNN and SNB, owing to
506 increasing emissions of VOCs and NO_x, while at OBI increasing O_3 and decreasing O_x trends arise
507 from the local decrease of NO emissions from automobiles.
508
509 The O_3 seasonal cycles are driven by temporal variations of precursor emissions and meteorology. The
510 largest and lowest AV_d are observed in summer and winter, respectively, for all sites, while the largest
511 values correspond to STA result of stagnant air masses. Annual cycles at all sites peak in spring and
512 through in winter, respectively, with a downward spike during summer caused by high winds that
513 disperse O_3, increase the boundary layer height, and low rainfall. Decreases in O_3 precursor emissions
514 during the economic crisis experienced in the country between 1994-1996, caused significant decline
515 trends in AV_s from 1993 to 1997 or 1998, depending on site, following by increasing trends in AV_s
516 derived of the recovery of the economy, which is underlined by the greatest increase of AV_s observed
517 at the industrial site SNN.
518
519 At all metropolitan areas, O_3 peaks after mid-day and dips before sunrise, though the peak value for
520 the MCMA occurs around an hour earlier than for the MMA and GMA caused by the accelerated photo-
521 chemical production of O_3 during late morning. Larger AV_d are seen at MCMA than at GMA and MMA
522 related to the relative emissions of the O_3 precursors, VOCs and NO_x. Non-significant differences at
523 any of the metropolitan areas between O_3 AV_d during weekends and weekdays are observed. This lack
524 of a weekend effect is understood to be likely due to weekday O_3 production being limited by VOCs
525 and inhibited by NO_x; reductions in VOCs emissions alone could reduce O_3 mixing ratios, whereas
526 reductions in NO_x may lead to increased O_3 mixing ratios.
527
528 A significant increasing trend of 0.20 ppb O_3 yr^{-1} within the MMA contrasts within a significant
529 decreasing trend of -0.71 ppb O_3 yr^{-1} within the MCMA during 1993-2014. A non-significant trend
530 evident within the GMA during 1996-2014, reflects long-term trends in VOC and NO_x emissions.
531 According to the long-term trends in O_3 for the MMA, the number of exceedances of the air quality
532 standards will very likely increase as result of increasing precursor emissions. This emphasises the
533 need for more stringent control of emissions in order to improve air quality within the MMA.
534

535 **5. Acknowledgments**

536 This research was supported by Tecnologico de Monterrey through the Research Group for Energy
537 and Climate Change (Grant 0824A0104 and 002EICIR01). Grateful acknowledgements are made to
538 the Secretariat for Sustainable Development of the Nuevo Leon State, the Secretariat for the
539 Environment of Mexico City and the Secretariat for the Environment and Territorial Development of the
540 Jalisco State for the public domain records. We gratefully thank the NOAA Air Resources Laboratory
541 (ARL) for provision of the HYSPLIT model and READY website (http://www.ready.noaa.gov). The
542 authors acknowledge Dr. Sigfrido Iglesias for providing imputed O_3 and NO_x data for the MMA time-

series. We are also grateful to Professor Paul Monks and Professor Richard Derwent for encouraging comments on an earlier version of the manuscript.

6. References

Agudelo-Castaneda, D. M., and Teixeira, E. C.: Time-series analysis of surface ozone and nitrogen oxides concentrations in an urban area at Brazil, Atmos. Pollut. Res., 5, 411-420, doi:10.5094/APR.2014.048, 2014.

Akimoto, H., Mori, Y., Sasaki, K., Nakanishi, H., Ohizumi, T., and Itano, Y.: Analysis of monitoring data of ground-level ozone in Japan for long-term trend during 1990-2010: Causes of temporal and spatial variation, Atmos. Environ., 102, 302-310, doi:10.1016/j.atmosenv.2014.12.001, 2015.

Atkinson, R.: Atmospheric chemistry of VOCs and NO_x. Atmos. Environ., 34, 2063-2101, doi:10.1016/S1352-2310(99)00460-4, 2000.

Benítez-García, S. E., Kanda, I., Wakamatsu, S., Okazaki, Y., and Kawano, M.: Analysis of criteria air pollutant trends in three Mexican metropolitan areas, Atmosphere, 5, 806-829, doi:10.3390/atmos5040806, 2014.

Bigi, A., and Harrison, R. M.: Analysis of the air pollution climate at a central urban background site, Atmos. Environ., 44, 2004-2012, doi:10.1016/j.atmosenv.2010.02.028, 2010.

Butler, T. M., Stock, Z. S., Russo, M. R., Denier Van Der Gon, H. A. C., and Lawrence, M. G.: Megacity ozone air quality under four alternative future scenarios, Atmos. Chem. Phys., 12, 4413-4428, doi:10.5194/acp-12-4413-2012, 2012.

Carslaw, D. C., and Ropkins, K.: openair - An R package for air quality data analysis, Environ. Model. Soft., 27-28, 52-61, doi:10.1016/j.envsoft.2011.09.008, 2012.

Carslaw, D. C.: The openair manual - open-source tools for analysing air pollution data, Manual for version 1.1-4, King's College London, 2015.

Chen, Z., Barros, C. P., and Gil-Alana, L. A.: The persistence of air pollution in four mega-cities of China, Habitat Int., 56, 103-108, doi:10.1016/j.habitatint.2016.05.004, 2016.

Cleveland, R. B., Cleveland, W. S., McRae, J., and Terpenning, I.: STL: A seasonal-trend decomposition procedure based on Loess, J. Off. Stats., 6, 3-33, 1990.

Cooper, O. R., Gao, R. -S., Tarasick, D., Leblanc, T., and Sweeney, C.: Long-term ozone trends at rural ozone monitoring sites across the United States, 1990-2010, J. Geophys. Res., 117, doi:10.1029/2012JD018261, 2012.

Cooper, O. R., Parrish, D. D., Ziemke, J., Balashov, N. V., Cupeiro, M., Galbally, I. E., Gilge, S., Horowitz, L., Jensen, N. R., Lamarque, J. -F., Naik, V., Oltmans, S. J., Schwab, J., Shindell, D. T., Thompson, A. M., Thouret, V., Wang, Y., and Zbinden, R. M.: Global distribution and trends of tropospheric ozone: An observation-based review. Elem. Sci. Anth., 2, doi: 10.12952/journal.elementa.000029, 2014.

Dentener, F., Stevenson, D., Cofala, J., Mechler, R., Amann, M., Bergamaschi, P., Raes, F., and Derwent, R.: The impact of air pollutant and methane emission controls on tropospheric ozone and radiative forcing: CTM calculations for the period 1990-2030, Atmos. Chem. Phys., 5, 1731-1755, doi:10.5194/acp-5-1731-2005, 2005.

Derwent, R. G., Manning, A. J., Simmonds, P. G., Spain, T. G., and O'Doherty, S.: Analysis and interpretation of 25 years of ozone observations at the Mace Head atmospheric research station on the Atlantic Ocean coast of Ireland from 1987 to 2012, Atmos. Environ., 80, 361-368, doi:10.1016/j.atmosenv.2013.08.003, 2013.

587 Domínguez-López, D., Vaca, F., Hernández-Ceballos, M. A., and Bolívar, J. P.: Identification and
588 characterisation of regional ozone episodes in the southwest of the Iberian Peninsula, Atmos. Environ.,
589 103, 276-288, doi:10.1016/j.atmosenv.2014.12.050, 2015.

590 Durbin, J., and Koopman, S. J.: Time Series Analysis by State Space Methods, Oxford University
591 Press, Oxford UK, 2nd Edition, 2012.

592 Fiore, A. M., Jacob, D. J., Logan, J. A., and Yin, J. H.: Long-term trends in ground level ozone over the
593 contiguous United States, 1980-1995, J. Geophys. Res., 103(D1), 1471-1480, doi:
594 10.1029/97JD03036, 1998.

595 Gallardo, L., Jorquera, H., and Molina, L. T.: Tackling challenges in assessing air quality over South
596 America, Eos, 93, 228, doi:10.1029/2012EO240005, 2012.

597 González-Santiago, O., Badillo-Castañeda, C. T., Kahl, J. D. W., Ramírez-Lara, E., and Balderas-
598 Renteria, I.: Temporal analysis of PM10 in Metropolitan Monterrey, México, J. Air Waste Manage, 61,
599 573-579, doi: 10.3155/1047-3289.61.5.573, 2011.

600 Guicherit, R., and Roemer, M.: Tropospheric ozone trends, Chemosphere, 2, 167-183,
601 doi:10.1016/S1465-9972(00)00008-8, 2000.

602 Hernández-Paniagua, I. Y., Lowry, D., Clemitshaw, K. C., Fisher, R. E., France, J. L., Lanoisellé, M.,
603 Ramonet, M., and Nisbet, E. G.: Diurnal, seasonal, and annual trends in atmospheric CO2 at
604 southwest London during 2000-2012: Wind sector analysis and comparison with Mace Head, Ireland,
605 Atmos. Environ., 105, 138-147, doi: 10.1016/j.atmosenv.2015.01.02, 2015.

606 INE (Instituto Nacional de Ecologia): Inventario de emisiones de la Zona Metropolitana de Guadalajara
607 1995, available at: http://www2.ine.gob.mx/publicaciones/libros/235/cap7.html, last access: 20 May
608 2016, 1997a.

609 INE (Instituto Nacional de Ecologia): Inventario de Emisiones de la Zona Metropolitana de Monterrey
610 1995, available at: http://www2.inecc.gob.mx/publicaciones/libros/234/cap6.html, last access: 20 May
611 2016, 1997b.

612 INE-SEMARNAT (Instituto Nacional de Ecologia-Secretaria del Medio Ambiente y Recursos
613 Naturales): Inventario Nacional de Emisiones 1999, México, D.F., available at:
614 http://www.inecc.gob.mx/dica/548-calaire-inem-1999, last access: 20 May 2016, 2006.

615 INE (Instituto Nacional de Ecologia): Cuarto almanaque de datos y tendencias de la calidad del aire en
616 20 ciudades mexicanas 2000-2009, INE-SEMARNAT, México, D.F., 405 pp., 2011.

617 INEGI (National Institute of Statistics and Geography): XIII Censo General de

618 Población y Vivienda 2010, México, available at: http://www.censo2010.org.mx/, last Access: 22 May
619 2016, 2010.

620 INEGI (National Institute of Statistics and Geography): México en Cifras, México, available at:
621 http://www3.inegi.org.mx/sistemas/mexicocifras/default.aspx?e=19, last access: 22 May 2016, 2015.

622 IPCC: Climate Change 2013: The Physical Science Basis. Contribution of Working Group I to the Fifth
623 Assessment Report of the Intergovernmental Panel on Climate Change, 2013. [Stocker, T.F., D. Qin,
624 G.-K. Plattner, M. Tignor, S.K. Allen, J. Boschung, A. Nauels, Y. Xia, V. Bex and P.M. Midgley (eds.)].
625 Cambridge University Press, Cambridge, United Kingdom and New York, NY, USA, 1535 pp., 2013.

626 Jaimes, P. M., Bravo, A. H., Sosa, E. R., Cureño, G. I., Retama, H. A., Granados, G. G., and Becerra,
627 A. E.: Surface ozone concentration trends in Mexico City Metropolitan Area, in: Proceedings of the Air
628 and Waste Management Association's Annual Conference and Exhibition AWMA, San Antonio, Texas,
629 19-22 June 2012, 3, 2273-2284, 2012.

630 Jenkin, M. E., and Clemitshaw, K. C.: Ozone and other secondary photochemical pollutants: chemical
631 processes governing their formation in the planetary boundary layer, Atmos. Environ., 34(16), 2499-
632 2527, doi:10.1016/S1352-2310(99)00478-1, 2000.

633 Kleanthous, S., Vrekoussis, M., Mihalopoulos, N., Kalabokas, P., and Lelieveld, J.: On the temporal
634 and spatial variation of ozone in Cyprus, Sci. Total Environ., 476-477, 677-687,
635 doi:10.1016/j.scitotenv.2013.12.101, 2014.

636 Kumar, A., Wu, S., Weise, M. F., Honrath, R., Owen, R. C., Helmig, D., Kramer, L., Val Martin, M., and
637 Li, Q.: Free-troposphere ozone and carbon monoxide over the North Atlantic for 2001-2011, Atmos.
638 Chem. Phys., 13, 12537-12547, doi:10.5194/acp-13-12537-2013, 2013.

639 Lelieveld, J., and Dentener, F. J.: What controls tropospheric ozone?, J. Geophys. Res., 105(D3),
640 3531-3551, doi:10.1029/1999JD901011, 2000.

641 Lelieveld, J., Evans, J. S., Fnais, M., Giannadaki, D., and Pozzer, A.: The contribution of outdoor air
642 pollution sources to premature mortality on a global scale, Nature Letts., 15371,
643 doi:10.1038/nature15371, 2015.

644 Logan, J. A., Megretskaia, I. A., Miller, A. J., Tiao, G. C., Choi, D., Zhang, L., Stolarski, R. S., Labow,
645 G. J., Hollandsworth, S. M., Bodeker, G. E., Claude, H., De Muer, D., Kerr, J. B., Tarasick, D. W.,
646 Oltmans, S. J., Johnson, B., Schmidlin, F., Staehelin, J., Viatte, P., and Uchino, O.: Trends in the
647 vertical distribution of ozone: A comparison of two analyses of ozonesonde data, J. Geophys. Res.,
648 104(D21), 26373-26399, doi:10.1029/1999JD900300, 1999.

649 Logan, J. A., Staehelin, J., Megretskaia, I. A., Cammas, J.-P., Thouret, V., Claude, H., De Backer, H.,
650 Steinbacher, M., Scheel, H.-E., Stübi, R., Fröhlich, M., and Derwent, R.: Changes in ozone over
651 Europe: Analysis of ozone measurements from sondes, regular aircraft (MOZAIC) and alpine surface
652 sites, J. Geophys. Res., 117(D9), doi: 10.1029/2011JD016952, 2012.

653 Molina, L. T., Madronich, S., Gaffney, J. S., Apel, E., de Foy, B., Fast, J., Ferrare, R., Herndon, S.,
654 Jimenez, J. L., Lamb, B., Osornio-Vargas, A. R., Russell, P., Schauer, J. J., Stevens, P. S., Volkamer,
655 R., and Zavala, M.: An overview of the MILAGRO 2006 Campaign: Mexico City emissions and their
656 transport and transformation, Atmos. Chem. Phys., 10, 8697-8760, doi:10.5194/acp-10-8697-2010,
657 2010.

658 Molina, M. J., and Molina, L. T.: Megacities and atmospheric pollution, J. Air Waste Manage., 54, 644-
659 680, doi:10.1080/10473289.2004.10470936, 2004.

660 Monks, P. S.: A review of the observations and origins of the spring ozone maximum, Atmos. Environ.,
661 34, 3545-3561, doi:10.1016/S1352-2310(00)00129-1, 2000.

662 Monks, P. S., Archibald, A. T., Colette, A., Cooper, O., Coyle, M., Derwent, R., Fowler, D., Granier, C.,
663 Law, K. S., Mills, G. E., Stevenson, D. S., Tarasova, O., Thouret, V., von Schneidemesser, E.,
664 Sommariva, R., Wild, O., and Williams, M. L.: Tropospheric ozone and its precursors from the urban to
665 the global scale from air quality to short-lived climate forcer, Atmos. Chem. Phys., 15, 8889-8973,
666 doi:10.5194/acp-15-8889-2015, 2015.

667 Munir, S., Habeebullah, T. M., Seroji, A. R., Gabr, S. S., Mohammed, A. M. F., and Morsy, E. A.:
668 Quantifying temporal trends of atmospheric pollutants in Makkah (1997-2012), Atmos. Environ., 77,
669 647-655, doi:10.1016/j.atmosenv.2013.05.075, 2013.

670 Oltmans, S. J., Lefohn, A. S., Harris, J. M., Galbally, I., Scheel, H. E., Bodeker, G., Brunke, E., Claude,
671 H., Tarasick, D., Johnson, B. J., Simmonds, P., Shadwick, D., Anlauf, K., Hayden, K., Schmidlin, F.,
672 Fujimoto, T., Akagi, K., Meyer, C., Nichol, S., Davies, J., Redondas, A., and Cuevas, E.: Long-term
673 changes in tropospheric ozone, Atmos. Environ., 40, 3156–3173, doi:10.1016/j.atmosenv.2006.01.029,
674 2006.

675 Ordóñez, C., Mathis, H., Furger, M., Henne, S., Hüglin, C., Staehelin, J., and Prévôt, A. S. H.: Changes
676 of daily surface ozone maxima in Switzerland in all seasons from 1992 to 2002 and discussion of
677 summer 2003, Atmos. Chem. Phys., 5, 1187-1203, doi:10.5194/acp-5-1187-2005, 2005.

ProAire-AMM (Programa de Gestión para Mejorar la Calidad del Aire del Área Metropolitana de Monterrey 2008-2012), SEMARNAT, Gobierno del estado de Nuevo León, available at: http://www.semarnat.gob.mx/archivosanteriores/temas/gestionambiental/calidaddelaire/Documents/Calidad%20del%20aire/Proaires/ProAires_Vigentes/6_ProAire%20AMM%202008-2012.pdf, last access: 22 May 2016, 2008.

ProAire-Jalisco (Programa para Mejorar la Calidad del Aire Jalisco 2011-2020), Secretaria de Medio Ambiente para el Desarrollo Sustentable, Gobierno de Jalisco, available at: http://www.semarnat.gob.mx/archivosanteriores/temas/gestionambiental/calidaddelaire/Documents/Calidad%20del%20aire/Proaires/ProAires_Vigentes/ProAire_Jalisco_2011-2020_Ver_10.pdf, last access: 23 May 2016, 2011.

ProAire-ZMVM (Programa para mejorar la calidad del aire de la Zona Metropolitana del Valle de México 2011-2020), Gobierno del Estado de México, Gobierno del Distrito Federal, SEMARNAT, available at:http://respiramexico.org.mx/wp-content/uploads/2015/07/proaire 2011-2020.pdf, last access: 23 May 2016, 2011.

Pugliese, S. C., Murphy, J. G., Geddes, J. A., and Wang, J. M.: The impacts of precursor reduction and meteorology on ground-level ozone in the Greater Toronto Area, Atmos. Chem. Phys., 14, 8197-8207, doi:10.5194/acp-14-8197-2014, 2014.

Qin, Y., Tonnesen, G. S., and Wang, Z.: Weekend/weekday differences of ozone, NO_x, Co, VOCs, PM_{10} and the light scatter during ozone season in southern California, Atmos. Environ., 38, 3069-3087, doi:10.1016/j.atmosenv.2004.01.035, 2004.

R Core Team: R: a Language and Environment for Statistical Computing, R

Foundation for Statistical Computing, Vienna, Austria, ISBN 3-900051-07-0, 2013, available at: www.R-project.org, last access: 23 May 2016, 2013.

Reinsel, G. C.: Elements of Multivariate Time Series Analysis. Springer-Verlag, New York, USA, 2nd Edition, 1997.

Revell, L. E., Tummon, F., Stenke, A., Sukhodolov, T., Coulon, A., Rozanov, E., Garny, H., Grewe, V. and Peter, T.: Drivers of the tropospheric ozone budget throughout the 21st century under the medium-high climate scenario RCP 6.0, Atmos. Chem. Phys., 15, 5887-5902, doi:10.5194/acp-15-5887-2015, 2015.

Rodríguez, S., Huerta, G., and Reyes, H.: A study of trends for Mexico City ozone extremes: 2001-2014, Atmosfera, 29, 107-120, doi:http://dx.doi.org/10.20937/ATM.2016.29.02.01, 2016.

Salmi, T., Määttä, A., Anttila, P., Ruoho-Airola, T. and Amnell, T.: Detecting trends of annual values of atmospheric pollutants by the Mann-Kendall test and Sen's slope estimates – the Excel template application MAKESENS, Publications on Air Quality Report code FMI-AQ-31, Helsinki, Finland, 31, 1-35, 2002.

Schultz, M., and Rast, S.: REanalysos of the TROpospheric chemical composition over the past 40 years, Emission Data Sets and Methodologies for Estimating Emissions, Work Package 1, Deliverable D1-6, available at: http://retro-archive.iek.fz-juelich.de/data/documents/reports/D1-6_final.pdf, last access: 14 Jul 2016, 2007.

SDS (Secretaria de Desarrollo Sustentable), Inventario de emisiones del Área Metropolitana de Monterrey 2013, personal communication, Monterrey, N.L. México, 4 Sep 2015.

SEDEMA (Secretaria del Medio Ambiente): INVENTARIO de Emisiones a la Atmosfera en la ZMVM 1996, available at: http://www.sedema.df.gob.mx/flippingbook/inventario-emisiones-1996/#p=1, last access: 20 May 2016, 1999.

SEDEMA (Secretaria del Medio Ambiente): Inventario de Emisiones Zona Metropolitana del Valle de Mexico 1998, available at: http://www.sedema.df.gob.mx/flippingbook/inventario-emisiones-zmvm1998/#p=75, last access: 20 May 2016, 2001.

SEDEMA (Secretaria del Medio Ambiente): Inventario de emisiones a la Atmosfera Zona Metropolitana del Valle de Mexico 2000, available at: http://www.sedema.df.gob.mx/flippingbook/inventario-emisiones-zmvm2000/, last access: 20 May 2016, 2003.

SEDEMA (Secretaria del Medio Ambiente): Inventario de emisiones de la Zona Metropolitana del Valle de Mexico 2002, available at: http://www.sedema.df.gob.mx/flippingbook/inventario-emisiones-zmvm-criterio2004/#p=1, last access: 20 May 2016, 2004.

SEDEMA (Secretaria del Medio Ambiente): Inventario de Emisiones Zona Metropolitana del Valle de Mexico 2004, available at: http://www.sedema.df.gob.mx/flippingbook/inventario-emisiones-zmvm-criterio2004/#p=1, last access: 20 May 2016, 2006.

SEDEMA (Secretaria del Medio Ambiente): Inventario de Emisiones de CONTAMINANTES CRITERIO 2006, available at: http://www.sedema.df.gob.mx/flippingbook/inventario-emisiones-zmvm-criterio2006/#p=1, last access: 20 May 2016, 2008.

SEDEMA (Secretaria del Medio Ambiente): Inventario de emisiones de contaminantes criterio de la ZMVM 2008, available at: http://www.sedema.df.gob.mx/flippingbook/inventario-emisiones-zmvm-criterio2008/#p=1, last access: 20 May 2016, 2010.

SEDEMA (Secretaria del Medio Ambiente): INVENTARIO DE EMISIONES DE LA ZONA METROPOLITANA DEL VALLE DE MEXICO CONTAMINANTES CRITERIO 2010, available at: http://www.sedema.df.gob.mx/flippingbook/inventario-em1isiones-zmvm-criterio-2010/#p=6, last access: 20 May 2016, 2012.

SEDEMA (Secretaria del Medio Ambiente): Inventario de emisiones contaminantes y de efecto invernadero, available at: http://www.sedema.df.gob.mx/flippingbook/inventario-emisioneszmvm2012/, last access: 20 May 2016, 2013.

SEDEMA (Secretaria del Medio Ambiente de la Ciudad de Mexico): Sistema de Monitoreo Atmosférico, http://www.aire.df.gob.mx/default.php, last access: 21 May 2016.

SEMADET (Secretaria de Medio Ambiente y Desarrollo Territorial Jalisco): http://semadet.jalisco.gob.mx/medio-ambiente/calidad-del-aire, last access: 21 May 2016.

SEMARNAT (Secretaria del Medio Ambiente y Recursos Naturales): Inventario Nacional de Emisiones 2005, México, D.F., available at: http://sinea.semarnat.gob.mx/sinae.php?process=UkVQT1JURUFET1I=&categ=1, last access: 22 May 2016, 2011.

SEMARNAT (Secretaria del Medio Ambiente y Recursos Naturales): Inventario Nacional de Emisiones 2008, México, D.F., available at: http://sinea.semarnat.gob.mx/ sinae.php?process=UkVQT1JURUFET1I=&categ=14, last access: 22 May 2016, 2014.

SENER (Secretaria de Energia): Estadísticas Energéticas Nacionales, México, available at: http://sie.energia.gob.mx/bdiController.do?action=temas, last Access: 4 November 2015, 2015.

SEMADET, (Secretaria de Medio Ambiente y Desarrollo Territorial): Inventario de Emisiones de Contaminantes Criterio del Estado de Jalisco 2008, SEMARNAT, Gobierno del Estado de Jalisco, available at: http://semadet.jalisco.gob.mx/sites/semadet.jalisco.gob.mx/files/inventario_de_emisiones_cc_jalisco_2008.pdf, last Access: 23 May 2016, 2014.

SEMADET, (Secretaria de Medio Ambiente y Desarrollo Territorial): Sistema de Monitoreo Atmosférico de Jalisco, available at: http://siga.jalisco.gob.mx/aire/ last access: 21 May 2016.

SDS (Secretaria de Desarrollo Sustentable): Sistema Integral de Monitoreo Ambiental, available at: http://aire.nl.gob.mx/, last access: 21 May 2016.

767 Sicard, P., Serra, R., and Rossello, P.: Spatiotemporal trends in ground-level ozone concentrations
768 and metrics in France over the time period 1999-2012, Environ. Res., 149, 122-144,
769 doi:10.1016/j.envres.2016.05.014, 2016.

770 Sierra, A., Vanoye, A. Y., and Mendoza, A.: Ozone sensitivity to its precursor emissions in
771 northeastern Mexico for a summer air pollution episode, J. Air Waste Manage., 63, 1221-1233,
772 doi:10.1080/10962247.2013.813875, 2013.

773 SMN (Servicio Meteorológico Nacional), available at: http://smn.cna.gob.mx/es/, last access: 21 May
774 2016.

775 Song, J., Lei, W., Bei, N., Zavala, M., de Foy, B., Volkamer, R., Cardenas, B., Zheng, J., Zhang, R.,
776 and Molina, L. T.: Ozone response to emission changes: a modeling study during the MCMA-
777 2006/MILAGRO Campaign, Atmos. Chem. Phys., 10, 3827-3846, doi:10.5194/acp-10-3827-2010,
778 2010.

779 Staehelin, J., and Schmid, W.: Trend analysis of tropospheric ozone concentrations utilizing the 20-
780 year data set of ozone balloon soundings over Payerne (Switzerland), Atmos. Environ., 25, 1739-1749,
781 doi:10.1016/0960-1686(91)90258-9, 1991.

782 Stephens, S., Madronich, S., Wu, F., Olson, J. B., Ramos, R., Retama, A., and Muñoz, R.: Weekly
783 patterns of México City's surface concentrations of CO, NO_x, PM_{10} and O_3 during 1986-2007, Atmos.
784 Chem. Phys., 8, 5313-5325, doi:10.5194/acp-8-5313-2008, 2008.

785 Stevenson, D. S., Dentener, F. J., Schultz, M. G., Ellingsen, K., van Noije, T. P. C., Wild, O., Zeng, G.,
786 Amann, M., Atherton, C. S., Bell, N., Bergmann, D. J., Bey, I., Butler, T., Cofala, J., Collins, W. J.,
787 Derwent, R. G., Doherty, R. M., Drevet, J., Eskes, H. J., Fiore, A. M., Gauss, M., Hauglustaine, D. A.,
788 Horowitz, L. W., Isaksen, I. S .A., Krol, M. C., Lamarque, J.-., Lawrence, M. G., Montanaro, V., Müller,
789 J.-., Pitari, G., Prather, M. J., Pyle, J. A., Rast, S., Rodriguez, J. M., Sanderson, M. G., Savage, N. H.,
790 Shindell, D. T., Strahan, S. E., Sudo, K., and Szopa, S.: Multimodel ensemble simulations of present-
791 day and near-future tropospheric ozone. J. Geophys. Res., D08301, doi: 10.1029/2005JD006338,
792 2006.

793 Tang, G., Li, X., Wang, Y., Xin, J., and Ren, X.: Surface ozone trend details and interpretations in
794 Beijing, 2001-2006, Atmos. Chem. Phys., 9, 8813-8823, doi:10.5194/acp-9-8813-2009, 2009.

795 Tiwari, A. K., Suresh, K. G., Arouri, M., and Teulon, F.: Causality between consumer price and
796 producer price: Evidence from Mexico. Economic Modelling, 36, 432-440,
797 doi:10.1016/j.econmod.2013.09.050, 2014.

798 van der A, R. J., H. J. Eskes, K. F. Boersma, T. P. C. van Noije, M. Van Roozendael, I. De Smedt, D.
799 H. M. U. Peters, and Meijer, E. W.: Trends, seasonal variability and dominant NO_x source derived from
800 a ten year record of NO_2 measured from space, J. Geophys. Res., 113, D04302,
801 doi:10.1029/2007JD009021, 2008.

802 Vingarzan, R.: A review of surface ozone background levels and trends, Atmos. Environ., 38, 3431-
803 3442, doi:10.1016/j.atmosenv.2004.03.030, 2004.

804 Volkamer, R., Sheehy, P., Molina, L. T., and Molina, M. J.: Oxidative capacity of the Mexico City
805 atmosphere-Part 1: A radical source perspective, Atmos. Chem. Phys., 10, 6969-6991,
806 doi:10.5194/acp-10-6969-2010, 2010.

807 Wang, T., Wei, X. L., Ding, A. J., Poon, C. N., Lam, K. S., Li, Y. S., Chan, L. Y., and Anson, M.:
808 Increasing surface ozone concentrations in the background atmosphere of Southern China, 1994–
809 2007, Atmos. Chem. Phys., 9, 6217-6227, doi:10.5194/acp-9-6217-2009, 2009.

810 Wang, Y., Konopka, P., Liu, Y., Chen, H., Müller, R., Plöger, F., Riese, M., Cai, Z., and Lü, D.:
811 Tropospheric ozone trend over Beijing from 2002-2010: Ozonesonde measurements and modeling
812 analysis, Atmos. Chem. Phys., 12, 8389-8399, doi:10.5194/acp-12-8389-2012, 2012.

West, J. J., Naik, V., Horowitz, L. W., and Fiore, A. M.: Effect of regional precursor emission controls on long-range ozone transport - Part 1: Short-term changes in ozone air quality, Atmos. Chem. Phys., 9, 6077-6093, doi:10.5194/acp-9-6077-2009, 2009.

Wilson, R. C., Fleming, Z. L., Monks, P. S., Clain, G., Henne, S., Konovalov, I. B., Szopa, S., and Menut, L.: Have primary emission reduction measures reduced ozone across Europe? An analysis of European rural background ozone trends 1996-2005, Atmos. Chem. Phys., 12, 437-454, doi:10.5194/acp-12-437-2012, 2012.

Wolff, G. T., Kahlbaum, D. F., and Heuss, J. M.: The vanishing ozone weekday/weekend effect, J. Air Waste Manage., 63, 292-299, doi:10.1080/10962247.2012.749312, 2013.

World Health Organization: Ambient (outdoor) air quality and health, 2014 update, http://www.who.int/mediacentre/factsheets/fs313/en/, last access: 21 May 2016.

Xu, X., Lin, W., Wang, T., Yan, P., Tang, J., Meng, Z., and Wang, Y.: Long-term trend of surface ozone at a regional background station in eastern China 1991-2006: Enhanced variability, Atmos. Chem. Phys., 8, 2595-2607, doi:10.5194/acp-8-2595-2008, 2008.

Zellweger, C., Hüglin, C., Klausen, J., Steinbacher, M., Vollmer, M., and Buchmann, B.: Inter-comparison of four different carbon monoxide measurement techniques and evaluation of the long-term carbon monoxide time series of Jungfraujoch, Atmos. Chem. Phys., 9, 3491-3503, doi:10.5194/acp-9-3491-2009, 2009.

Zhang, Q., Streets, D. G., He, K., Wang, Y., Richter, A., Burrows, J. P., Uno, I., Jang, C. J., Chen, D., Yao, Z., and Lei, Y.: NOx emission trends for China, 1995-2004: The view from the ground and the view from space, J. Geophys. Res., D22306, doi:10.1029/2007JD008684, 2007.

Table 1. Air quality limit values stated in the Mexican legislation.

Pollutant	Mexican Official Standard	Limit value*
O_3 (ppb)	NOM-020-SSA1-1993	110 (1-h), 80 (8-h)[a,b]
	NOM-020-SSA1-2014	95 (1-h) , 70 (8-h)[a,b]
PM_{10} ($\mu g\ m^{-3}$)	NOM-025-SSA1-1993	75 (24-h), 40 (1-yr)
	NOM-025-SSA1-2014	50 (24h), 35 (1-yr)
$PM_{2.5}$ ($\mu g\ m^{-3}$)	NOM-025-SSA1-1993	45 (24-h), 12 (1-yr)
	NOM-025-SSA1-2014	30 (24-h), 10 (1-yr)
CO (ppm)	NOM-02-SSA1-1993	11 (8-h)[b]
NO_2 (ppm)	NOM-023-SSA1 -1993	0.21 (1-h)

*Average period.
[a]Not to be exceeded more than four times in a calendar year.
[b]Running average.

Atmos. Chem. Phys. Discuss., doi:10.5194/acp-2016-654, 2016
Manuscript under review for journal Atmos. Chem. Phys.
Published: 12 September 2016

Table 2. Site description, location and instrumentation used during 1993 to 2014 within the MMA.

Site	Code	Location	Elevation (m a.s.l.)	Site description
Guadalupe	GPE	25° 40.110' N, 100° 14.907' W	492	Urban background site in the La Pastora park, downwind of an industrial corridor surrounded by a highly populated area, 450 m from Pablo Rivas Rd.
San Nicolas	SNN	25° 44.727' N, 100° 15.301' W	476	Urban site surrounded by a large number of industries and residential areas, 450 m from Juan Diego Diaz de Beriagna Rd.
Obispado	OBI	25° 40.561' N, 100° 20.314' W	560	Urban site near the city centre of MMA, 250 m from Jose Eleuterio González Rd. and 250 m from Antonio L. Rodríguez Rd.
San Bernabe	SNB	25° 45.415' N, 100° 21.949' W	571	Urban site in a residential area downwind of an industrial area with high traffic volume, 140 m from Aztlan Rd.
Santa Catarina	STA	25° 40.542' N, 100° 27.901' W	679	Urban site downwind of industrial sources, 200 m from Manuel Ordoñez Rd.

Atmos. Chem. Phys. Discuss., doi:10.5194/acp-2016-654, 2016
Manuscript under review for journal Atmos. Chem. Phys.
Published: 12 September 2016

Table 3. Statistics of O_3 data in units of ppb at the 5 monitoring sites in the MMA during 1993-2014.

Year	GPE					SNN					OBI					SNB					STA				
	Min	AVG	SD	Median	Max	Min	AVG	SD	Median	Max	Min	AVG	SD	Median	Max	Min	AVG	SD	Median	Max	Min	AVG	SD	Median	Max
1993	0	23	17	20	130	2	31	16	28	113.5	0	31	21	26	181.5	0	31	19	27	118	0	30	23	23	182.5
1994	0	21	16	19	113.5	0	19	12	17	98.5	0	15	15	11	127	0	18	14	15	122.5	0	21	22	15	153
1995	0	24	16	22	103	0	19	12	17	98	0	14	11	13	104.5	0	20	15	17	109	0	24	21	19	130.5
1996	0	23	17	21	174	0	18	13	15	110	0	20	19	15	144	0	24	18	21	126.5	0	23	22	17	154
1997	0	22	18	19	185.5	0	18	14	16	94.5	0	19	18	15	153.5	0	23	18	20	134.5	0	23	24	17	174.5
1998	0	27	18	27	115.5	0	20	13	19	76.5	0	18	16	14	103.5	0	26	20	23	137	0	21	20	16	135.5
1999	NR	NR	NR	NR	NR	0	25	22	20	52	0	21	17	17	102.5	0	25	19	21	154.5	0	22	21	17	157
2000	0	15	13	13	105.5	0	18	13	15	78	0	16	14	12	107	0	25	19	20	141	0	20	21	13	122.5
2001	0	22	17	19	111	0	16	12	15	88	0	14	14	10	129	0	21	17	17	223.5	0	19	20	12	177.5
2002	0	26	19	22	114	0	21	15	19	109	0	21	18	16	123.5	0	25	19	22	129.5	0	21	21	15	143.5
2003	1	22	18	17	126	1	18	14	15	109	1	20	18	14	129	1	25	19	20	146	1	20	21	14	153
2004	0	25	19	22	144	0	23	17	19	145	0	23	21	17	175	0	28	21	24	137	0	23	24	16	164
2005	0	27	21	24	149	0	25	19	21	142	0	23	21	17	139	0	28	22	23	154	0	24	23	17	169
2006	0	27	21	24	172	0	25	19	21	146	0	25	21	19	165	0	28	22	23	161	0	23	22	16	173
2007	1	27	19	23	142	0	23	17	19	124	0	23	20	17	130	1	25	20	20	139	1	22	21	15	144
2008	0	28	21	23	134	1	25	18	20	124	0	24	21	19	135	1	27	21	22	138	0	25	22	18	153
2009	0	28	20	25	132	0	25	17	21	123	0	22	18	18	142	1	26	20	22	121	0	25	21	19	148
2010	1	26	19	23	134	1	23	17	19	136	1	22	19	18	138	1	26	20	21	125	1	24	21	18	148
2011	0	29	20	25	119	0	26	18	22	120	0	26	21	21	121	1	30	22	25	140	1	26	23	20	135
2012	0	26	18	23	132	1	25	16	22	107	0	23	19	20	120	0	27	20	24	126	0	23	19	19	135
2013	1	26	19	23	161	2	24	17	21	126	1	23	19	19	139	1	26	19	22	133	1	23	19	18	118
2014	1	24	19	20	139	2	23	17	19	136	1	21	19	17	134	2	26	21	21	140	1	27	23	21	155

NR: No records
AVG: Average.
SD: Standard deviation of the averages.

Atmos. Chem. Phys. Discuss., doi:10.5194/acp-2016-654, 2016
Manuscript under review for journal Atmos. Chem. Phys.
Published: 12 September 2016

Atmospheric Chemistry and Physics Discussions

Table 4. Average O_3 growth rates in ppb yr^{-1} for 1993-2014 calculated by wind sector at the 5 sites within the MMA.

Site	N	NE	E	SE	S	SW	W	NW
GPE	0.23[c]	0.16[b]	0.43[c]	0.55[c]	0.23[c]	0.15[c]	0.05[a]	0.11[a]
SNN	0.16[c]	0.06	0.36[c]	0.46[c]	0.08	-0.05	0.04	0.03
OBI	0.08[b]	0.22[c]	0.50[c]	0.66[c]	0.32[c]	0.18[c]	0.06	0.06
SNB	0.36[c]	0.43[c]	0.43[c]	0.16[a]	-0.09	-0.06	-0.04	0.00
STA	0.00	0.02	0.06	0.25[c]	0.08[a]	0.00	-0.05[a]	-0.02

[a]Level of significance $p < 0.1$.
[b]Level of significance $p < 0.05$.
[c]Level of significance $p < 0.001$.

Atmos. Chem. Phys. Discuss., doi:10.5194/acp-2016-654, 2016
Manuscript under review for journal Atmos. Chem. Phys.
Published: 12 September 2016

Atmospheric Chemistry and Physics Discussions

859 **Table 5.** Daily exceedances of the O_3 1-h average and 8-h running average NOM during
860 1993-2014 at the 5 sites within the MMA.

Year	1-h average					8-h running average				
	GPE	SNN	OBI	SNB	STA	GPE	SNN	OBI	SNB	STA
1993	6	1	26	5	41	7	0	43	10	74
1994	1	0	1	2	33	0	0	0	0	22
1995	0	0	0	0	7	0	0	0	0	0
1996	15	0	17	2	27	14	0	11	0	24
1997	9	0	12	11	56	9	0	4	5	63
1998	2	0	0	6	20	0	0	0	16	19
1999	NR	0	0	5	11	0	0	0	2	4
2000	0	0	0	4	13	0	0	0	5	16
2001	1	0	2	2	19	0	0	0	0	21
2002	2	0	4	2	13	13	0	9	7	19
2003	1	0	2	6	31	0	0	0	7	42
2004	10	2	17	10	52	17	1	20	26	55
2005	6	4	15	23	52	21	12	24	47	74
2006	23	9	17	13	18	40	8	27	15	20
2007	8	3	8	10	21	11	0	4	3	27
2008	6	7	17	21	40	25	15	38	50	79
2009	13	3	8	3	19	15	0	11	6	25
2010	5	5	11	13	31	9	5	22	22	30
2011	5	4	7	26	26	14	0	26	62	48
2012	4	0	3	8	3	2	0	0	16	3
2013	9	3	12	9	8	14	1	18	24	7
2014	10	7	9	10	38	8	0	6	19	80
Total	136	48	188	191	579	219	42	263	342	752

861 NR: No records
862

Atmos. Chem. Phys. Discuss., doi:10.5194/acp-2016-654, 2016
Manuscript under review for journal Atmos. Chem. Phys.
Published: 12 September 2016

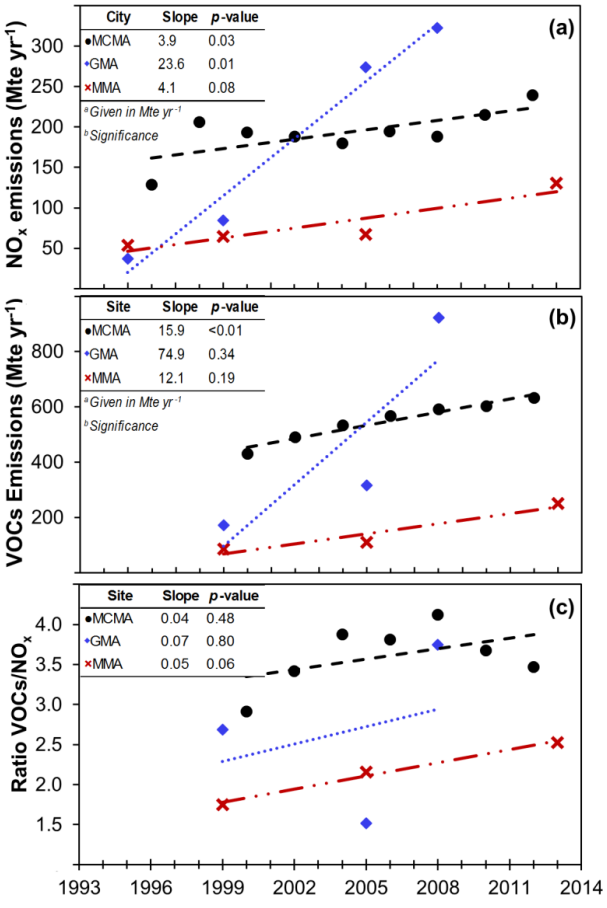

Fig. 1(a). Emissions trends for NO_x, (b). VOCs and (c) Ratios $VOCs/NO_x$ at MCMA, GMA and MMA during 1995-2013. Adapted from: INE, 1997a,b; SEDEMA, 1999; 2001; 2003; 2004; INE-SEMARNAT, 2006; SEDEMA, 2006; 2008; 2010; SEMARNAT, 2011; SEDEMA, 2012; 2013; SEMARNAT, 2014; SDS, 2015.

Atmos. Chem. Phys. Discuss., doi:10.5194/acp-2016-654, 2016
Manuscript under review for journal Atmos. Chem. Phys.
Published: 12 September 2016

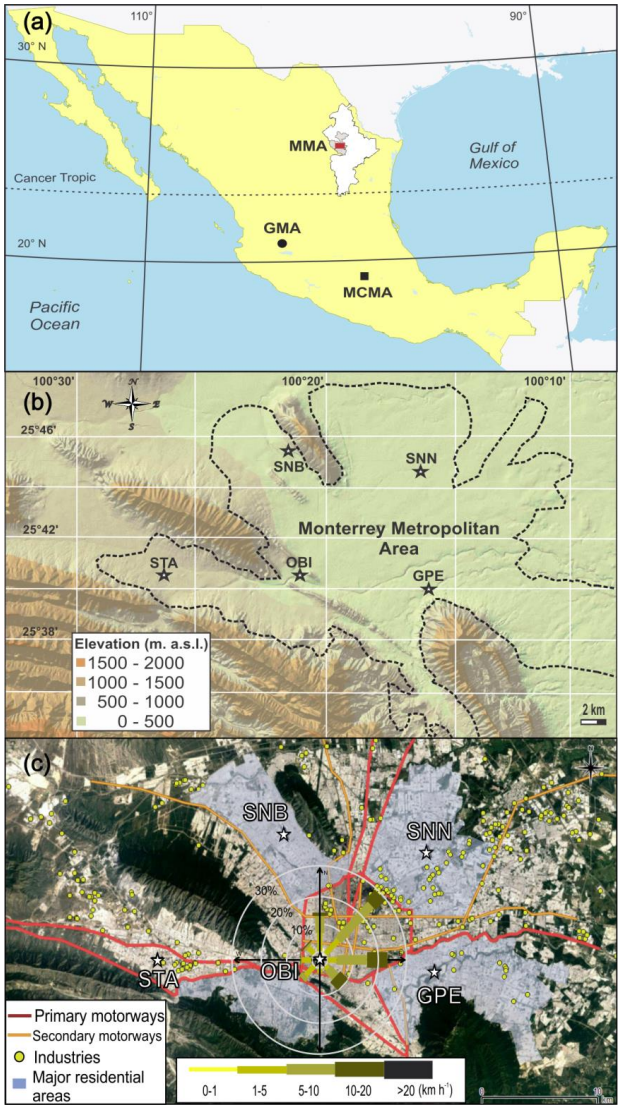

Fig. 2(a). The MMA, MCMA and GMA in the national context. **(b).** Topography of the MMA and distribution of the 5 monitoring sites over the area. **(c).** The 5 monitoring sites in relation to primary and secondary motorways, industries and major residential areas. The wind rose centred at the OBI site shows the average frequency of counts of measured wind direction occurrence from 1993 to 2014.

Atmos. Chem. Phys. Discuss., doi:10.5194/acp-2016-654, 2016
Manuscript under review for journal Atmos. Chem. Phys.
Published: 12 September 2016

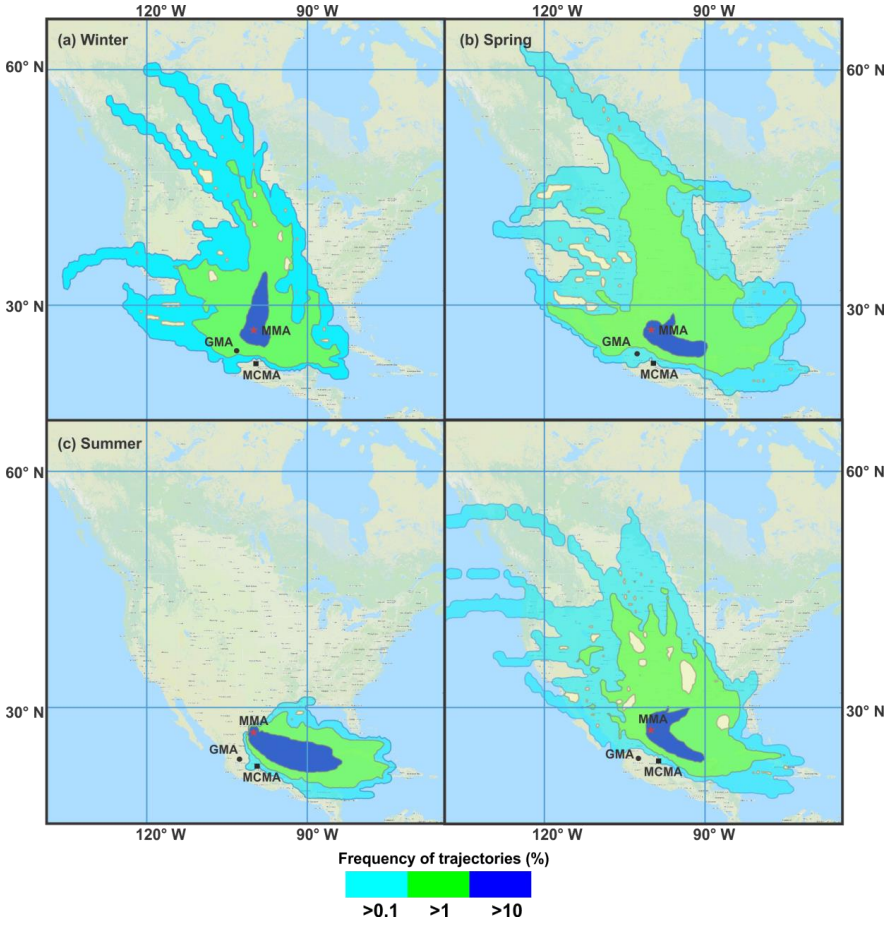

876

877 **Fig. 3.** HYSPLIT frequency plots of 96-h back trajectories from the MMA by season during
878 2014. Each panel represents 3-months of data, with a new trajectory represented every 6
879 hours.
880

Atmos. Chem. Phys. Discuss., doi:10.5194/acp-2016-654, 2016
Manuscript under review for journal Atmos. Chem. Phys.
Published: 12 September 2016

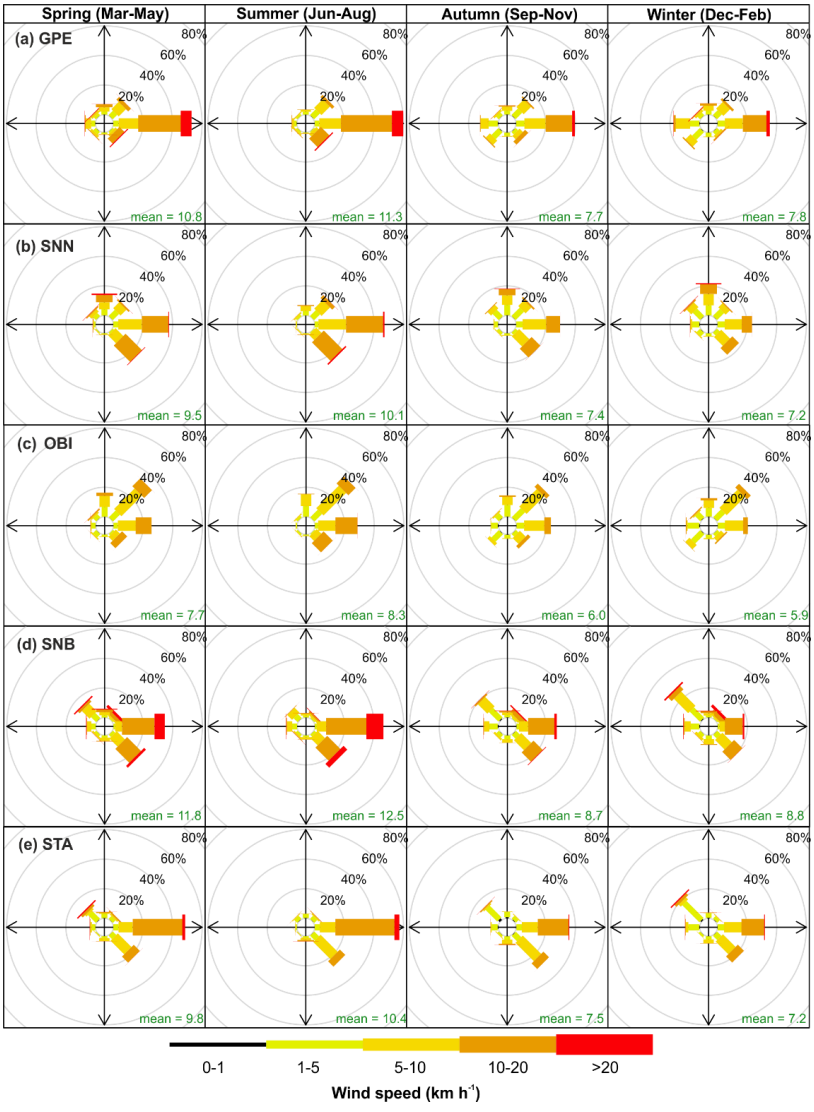

Fig. 4. Frequency of counts of measured wind direction occurrence by season and site within the MMA during 1993-2014.

Atmos. Chem. Phys. Discuss., doi:10.5194/acp-2016-654, 2016
Manuscript under review for journal Atmos. Chem. Phys.
Published: 12 September 2016

Atmospheric Chemistry and Physics Discussions

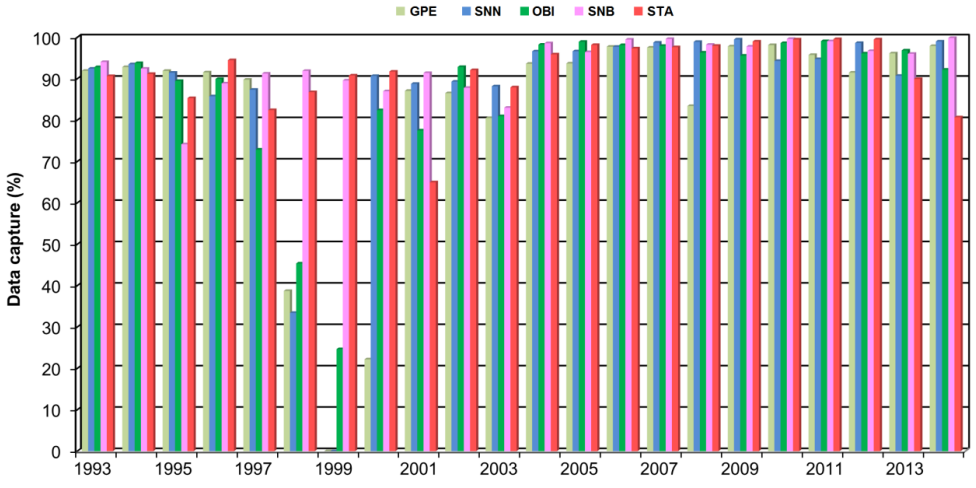

Fig. 5. Data capture of 1-h averages recorded for O_3 at the 5 monitoring sites within the MMA during 1993-2014.

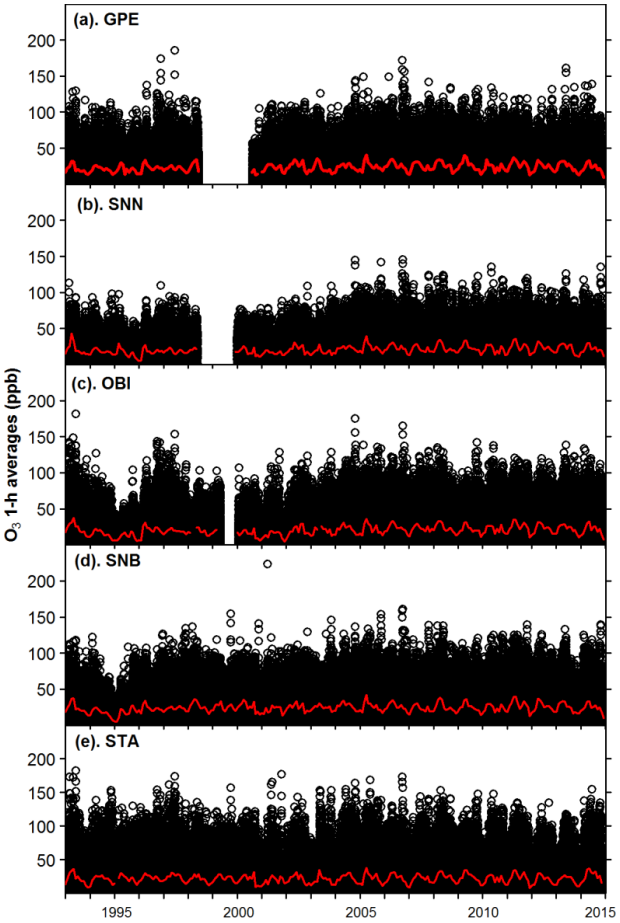

Fig. 6. 1-h averages of O_3 mixing ratios recorded from Jan 1993 to Dec 2014 within the MMA. The red line shows monthly averages of O_3 calculated from daily averages.

Atmos. Chem. Phys. Discuss., doi:10.5194/acp-2016-654, 2016
Manuscript under review for journal Atmos. Chem. Phys.
Published: 12 September 2016

Atmospheric Chemistry and Physics Discussions

892

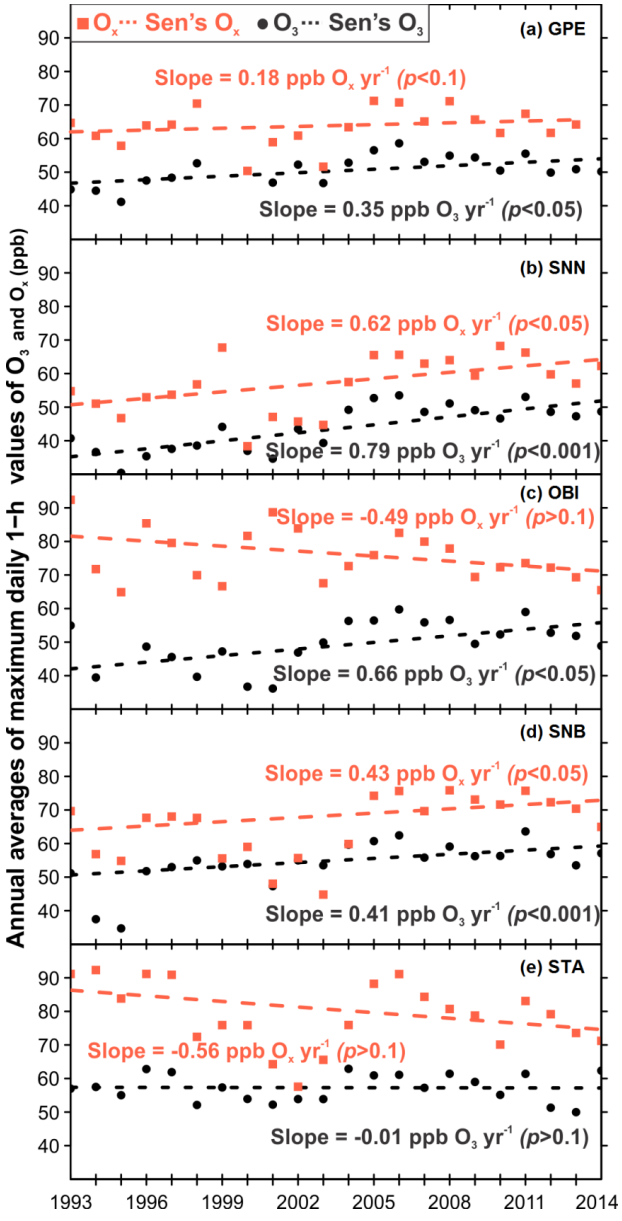

893

894 **Fig. 7.** Long-term trends of maximum daily 1-h values O_3 and O_x observed during 1993-
895 2014 within the MMA.
896

Atmos. Chem. Phys. Discuss., doi:10.5194/acp-2016-654, 2016
Manuscript under review for journal Atmos. Chem. Phys.
Published: 12 September 2016

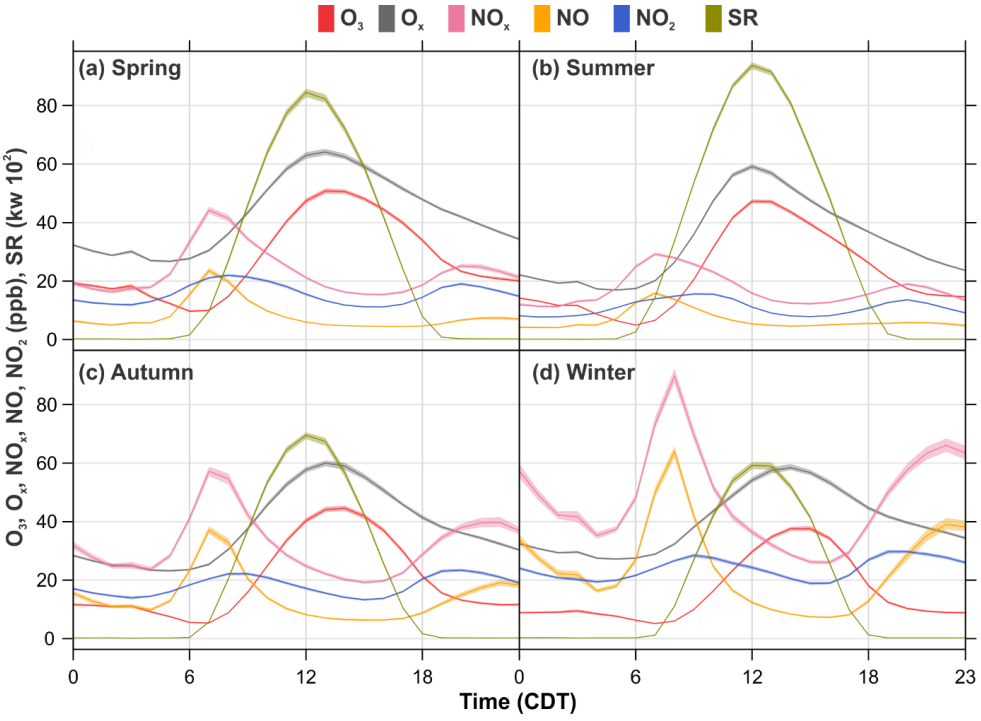

Fig. 8. Average daily profiles for O_3, O_x, NO_x, NO, NO_2 and SR within the MMA during 1993-2014. The shading shows the 95 % confidence intervals of the average.

Atmos. Chem. Phys. Discuss., doi:10.5194/acp-2016-654, 2016
Manuscript under review for journal Atmos. Chem. Phys.
Published: 12 September 2016

Atmospheric Chemistry and Physics Discussions

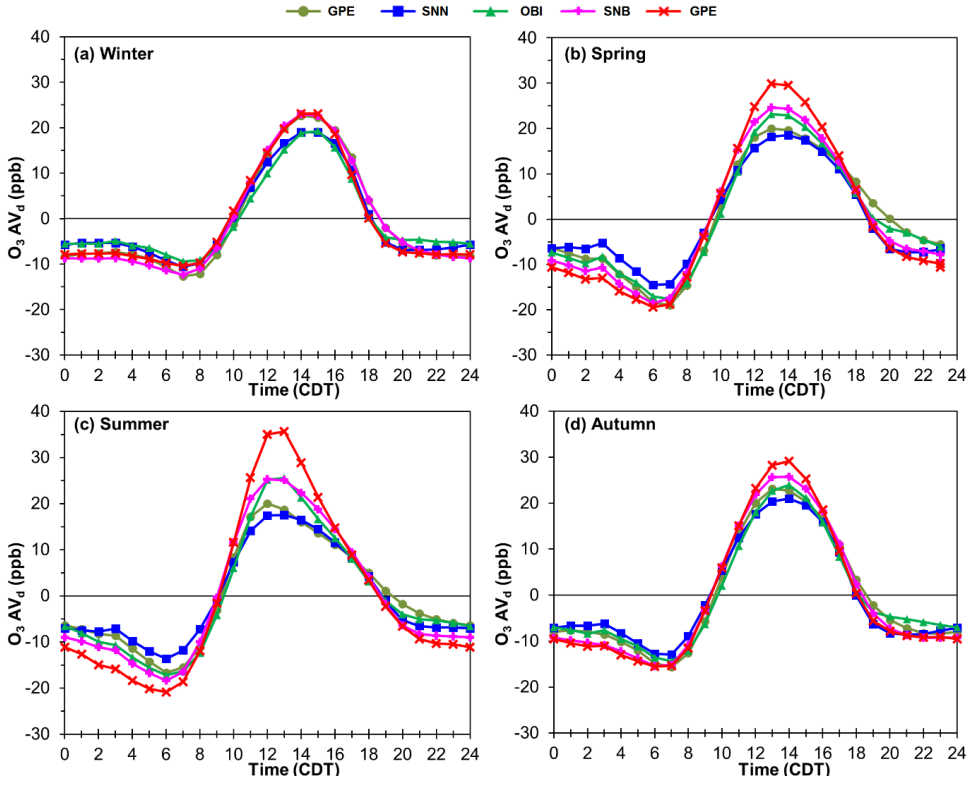

Fig. 9. O_3 de-trended daily profiles by season observed within the MMA during 1993-2014.

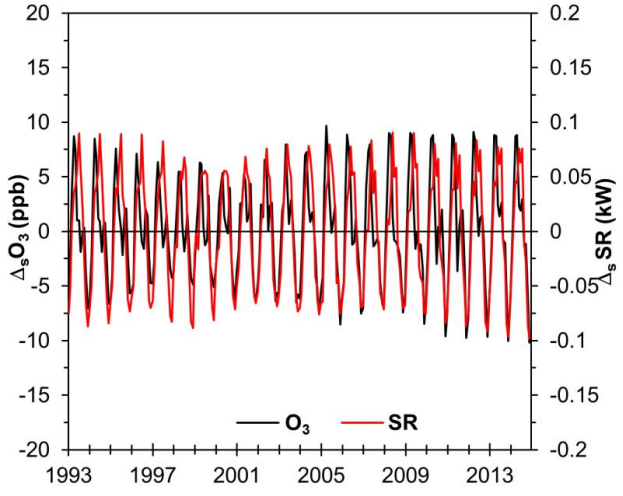

Fig. 10. Seasonal variations in O_3 mixing ratios and SR constructed from filtered data using the STL technique developed by Cleveland et al. (1990).

Atmos. Chem. Phys. Discuss., doi:10.5194/acp-2016-654, 2016
Manuscript under review for journal Atmos. Chem. Phys.
Published: 12 September 2016

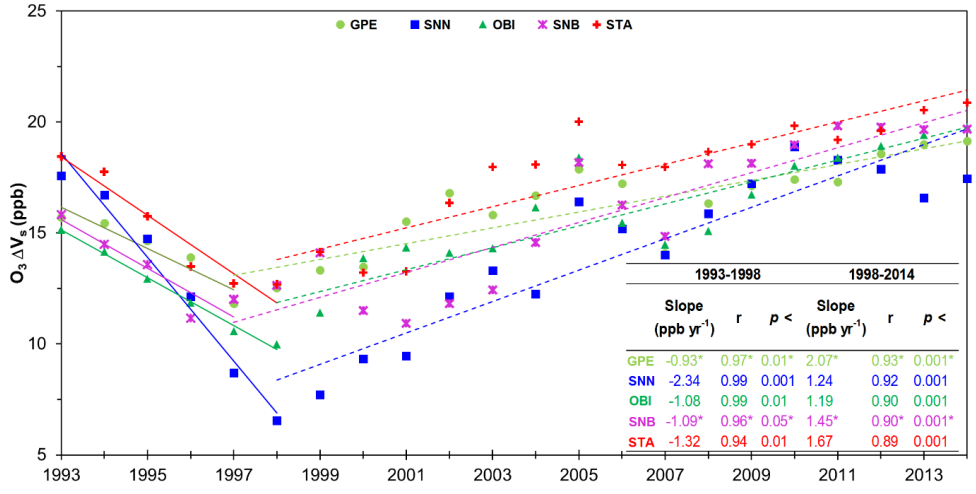

Fig. 11. AV_s and trends of AV_s of O_3 recorded within the MMA from 1993-2014. The decline in AV_s observed is due to the economic crisis experienced at the country during 1994-1996, followed by persistent increases in AV_s since 1998.

Atmos. Chem. Phys. Discuss., doi:10.5194/acp-2016-654, 2016
Manuscript under review for journal Atmos. Chem. Phys.
Published: 12 September 2016

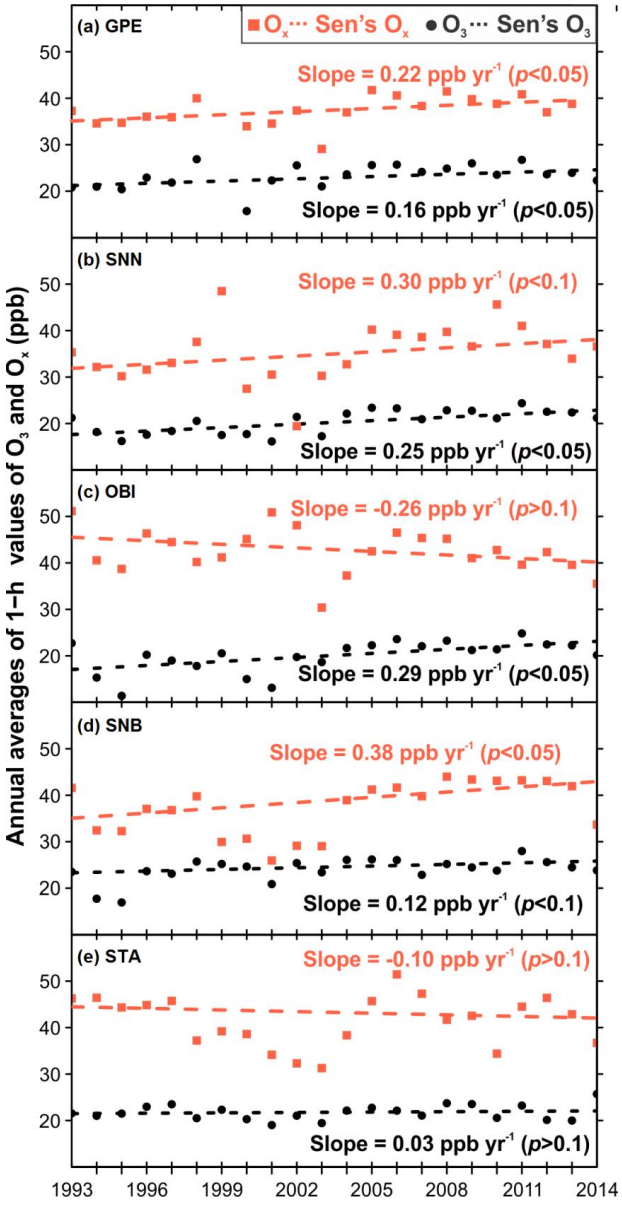

Fig. 12. Long-term trends of de-seasonalised data for O_3 recorded at the 5 sites within the MMA during 1993-2014.

Atmos. Chem. Phys. Discuss., doi:10.5194/acp-2016-654, 2016
Manuscript under review for journal Atmos. Chem. Phys.
Published: 12 September 2016

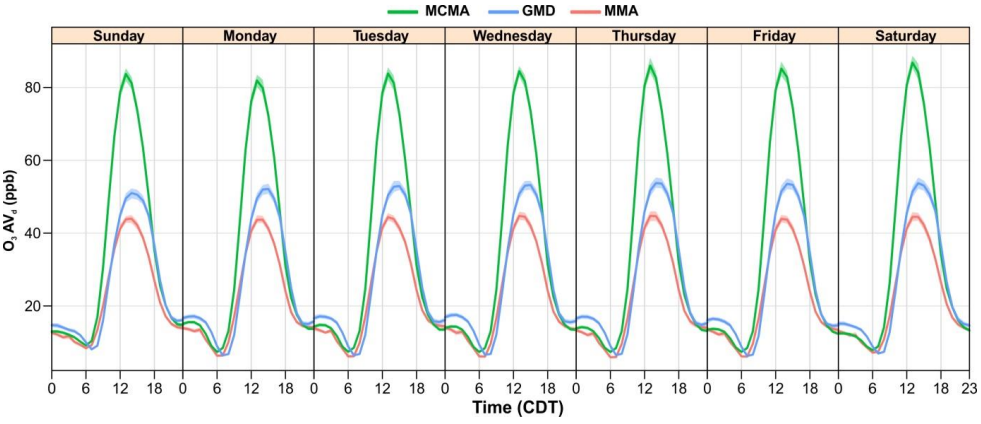

Fig. 13. Average weekly cycles of O_3 at the three major metropolitan areas in Mexico during 1993-2014 for the MCMA and the MMA, and between 1996-2014 for the GMA. The shading shows the 95% confidence intervals of the average.

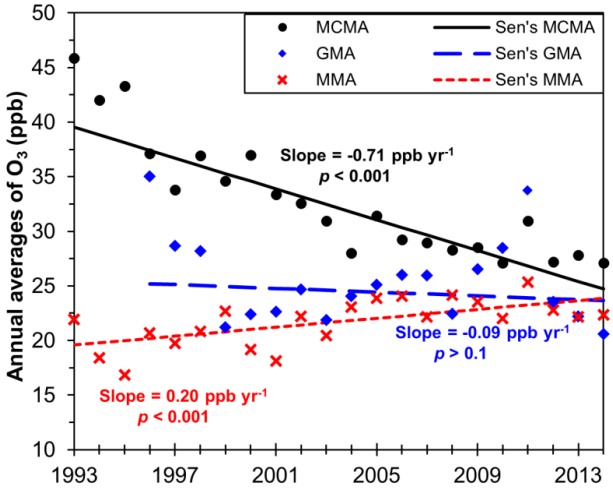

Fig. 14. Long-term trends of O_3 for the MCMA and MMA during 1993-2014, and for the GMA during 1996-2014.